TU-604
DPNU-00-34
hep-ph/0010260
October, 2000

Top Mode Standard Model with Extra Dimensions

Michio HASHIMOTO*, Masaharu TANABASHI†

Department of Physics, Tohoku University
Sendai 980-8578, Japan

Koichi YAMAWAKI‡

Department of Physics, Nagoya University
Nagoya 464-8602, Japan

Abstract

We critically examine a version of the top mode standard model recently cast in extra dimensions by Arkani-Hamed, Cheng, Dobrescu, and Hall, based on the (improved) ladder Schwinger-Dyson (SD) equation for the D-($= 6, 8$-)-dimensional gauge theories. We find that the bulk QCD cannot have larger coupling beyond the *non-trivial ultraviolet (UV) fixed point*, the existence of which is supported by a recent lattice analysis. The coupling strength at the fixed point is evaluated by using the one-loop renormalization group equation. It is then found that, in a version with only the third family (as well as the gauge bosons) living in the D-dimensional bulk, the critical (dimensionless) coupling for dynamical chiral symmetry breaking to occur is larger than the UV fixed point of the bulk QCD coupling for $D = 6$, while smaller for $D = 8$. We further find that the *improved* ladder SD equation in D dimensions has an *approximate scale-invariance* due to the *running* of the coupling and hence has an *essential-singularity scaling* of the

*michioh@tuhep.phys.tohoku.ac.jp
†tanabash@tuhep.phys.tohoku.ac.jp
‡yamawaki@eken.phys.nagoya-u.ac.jp

"conformal phase transition," similar to Miransky scaling in the four-dimensional *ladder* SD equation with a *nonrunning* coupling. This essential-singularity scaling can resolve the fine-tuning even when the cutoff ("string scale") is large. Such a theory has a *large anomalous dimension* $\gamma_m = D/2 - 1$ and is expected to be free from the flavor-changing-neutral-current problem as in walking technicolor for $D = 4$. Furthermore, the induced bulk Yukawa coupling becomes finite even at infinite cutoff limit (in the formal sense), similarly to the renormalizability of the gauged Nambu-Jona-Lasinio model. Comments are made on the use of the "effective" coupling, which includes finite renormalization effects, instead of the $\overline{MS}$ running coupling in the improved ladder SD equation.

1 Introduction

The top quark condensate proposed by Miransky, Tanabashi and Yamawaki (MTY) [1, 2] and by Nambu [3] independently is a natural idea to account for the large mass of the top quark (t) on the weak-scale order in contrast with other quarks and leptons. The Higgs boson in the standard model (SM) emerges as a $\bar{t}t$ bound state and hence is closely connected with the top quark itself. Thus the model may be called the "top mode standard model (TMSM)" [2].

Actually, MTY introduced explicit four-fermion interactions [1, 2]

$$\mathcal{L}_{4f} = \frac{4\pi^2}{N_c \Lambda^2} \left[g_t (\bar{\psi}_L t_R)^2 + g_b (\bar{\psi}_L b_R)^2 + g^{(2)} \epsilon^{i,k} \epsilon^{j,l} (\bar{\psi}_L^i \psi_R^j)(\bar{\psi}_L^k \psi_R^l) + \text{h.c.} \right], \tag{1.1}$$

with $i(j,k,l) = t, b$ for top and bottom quarks, where $g_t, g_b, g^{(2)}$ are dimensionless four-fermion couplings, Λ is the cutoff, and N_c is the number of colors, and similarly for leptons as well as the first and second generations of quarks and leptons. While g_t is responsible for the top mass, the $g^{(2)}$ coupling is vital to the generation of the bottom mass without the problem of the axion. MTY further gave a concrete formulation based on the (improved) ladder Schwinger-Dyson (SD) equation for the QCD plus the four-fermion interaction (1.1), the gauged Nambu–Jona-Lasinio (NJL) model, and found that when

$$g_t > g_{crit} > g_b \tag{1.2}$$

only the top quark can condense, giving rise to the large top mass, while the bottom quark is kept massless, where g_{crit} is the critical coupling of the SD equation. As to the value of the top mass, MTY substituted the solution of the (improved) ladder SD equation into the Pagels-Stokar (PS) formula [4] for $F_\pi = 250$ GeV and predicted $m_t \simeq 250$GeV for the cutoff near the Planck scale [1, 2].

The model was further formulated in an elegant fashion by Bardeen, Hill, and Lindner (BHL) [5] in the SM language, based on the renormalization-group equation (RGE) and the compositeness condition. This essentially incorporates $1/N_c$ subleading effects disregarded by the MTY paper. The BHL model is in fact equivalent to the MTY model at $1/N_c$ leading order [6]. Such $1/N_c$-subleading effects reduced the above MTY value 250 GeV to 220 GeV, a somewhat smaller value but still on the order of the weak scale. Even this value, however, turned out to be a bit larger than the mass of the top quark observed later .

Quite recently, Arkani-Hamed, Cheng, Dobrescu, and Hall (ACDH) [7] proposed a very interesting version of the TMSM in six and eight dimensions, in which the third family fermion and the gauge bosons are put in the D-($= 6, 8$-)-dimensional bulk, while the first and second families are in the four-dimensional brane (3-brane). The model is largely based on the earlier papers [8, 9], which, motivated by the topcolor [10] and the top-seesaw model [11], proposed formulating the top quark condensate in the extra dimensions in the spirit of large scale compactification scenarios [12, 13]. ACDH argued that the D-dimensional SM gauge couplings become strong due to Kaluza-Klein

(KK) modes of the standard model gauge bosons and hence may naturally give rise to the effective four-fermion interactions *in D-dimensional bulk* which have the same structure as Eq.(1.1), with $g_t > g_{crit} > g_b$, the situation similar to the original TMSM, Eq.(1.2). [1] Moreover they argued that the top mass can be arranged to be a realistic value due to the effects of many KK modes of top quark even for the TeV scale cutoff, thus the model may be free from serious fine tuning as compared with the original TMSM having the cutoff near the Planck scale.

However, ACDH gave no dynamical arguments on whether dynamical symmetry breaking really takes place or not in their model. They made an ansatz that bulk strong gauge dynamics in the ultraviolet region near the cutoff ("string scale") can well be simulated by the D-dimensional *bulk four-fermion couplings* characterized by the cutoff scale. They then calculated the *relative strength* of the bulk attractive forces among various channels based on the most attractive channel (MAC) hypothesis [16] and argued that only the top coupling can be arranged to be above the critical coupling like Eq.(1.2) in the original mechanism of MTY. However, this would make sense only when these four-fermion couplings were near the critical coupling, the situation being what they simply assumed. In fact, there is no information on the strength of the bulk effective four-fermion couplings, which cannot be related in any definite manner to the bulk gauge coupling, while the latter is calculable through matching with the low-energy SM coupling in four dimensions (3-brane) at the compactification scale [17].

In this paper, we shall study the dynamical issues of the ACDH version of the TMSM, based on the (improved) ladder SD equation for the gauge theories in the bulk D $(= 6, 8)$ dimensions. As in ACDH [7], we here assume that the bulk anomaly may be cancelled by some stringy arguments like the Green-Schwarz mechanism. Then we present explicit solutions for the dynamical chiral symmetry breaking (DχSB) for D dimensions with their implications on the ACDH scenario and reveal some salient features of this dynamics for D dimensions.

We first discuss a *nontrivial ultraviolet (UV) fixed point* in the one-loop renormalization-group equation of the "truncated KK" effective theory [17] of D-dimensional non-Abelian gauge theories with compactified extra dimensions, in a manner similar to the analysis of $D = 4 + \epsilon$ $(0 < \epsilon \ll 1)$ gauge theories. Although such a fixed point cannot be justified for $\epsilon \sim \mathcal{O}(1)$ within the perturbative analysis, its existence is supported by a recent lattice calculation[28]. Assuming the nonperturbative existence of such a fixed point, we then evaluate the gauge coupling strength at the fixed point by using the one-loop RGE which was actually adopted by ACDH for their prediction of the top quark mass. In the bulk SM, QCD is the only non-Abelian gauge theory relevant to the DχSB. We then observe that *the D-dimensional bulk QCD coupling cannot grow over the fixed point value*, since at a certain compactification scale we match the bulk QCD coupling with the 3-brane QCD coupling, which is obviously small, and hence the phase must be in the weak coupling regime below the fixed point. The QCD coupling

[1] The previous studies in extra dimensions[8, 9, 14] were focused on the four-fermion interactions *in the 3-brane* in contrast to those in the ACDH model which are *in the D-dimensional bulk* [7, 15].

for the ACDH version of the TMSM for $D = 6, 8$ is actually evaluated by the truncated KK effective theory.

We next study the dynamical symmetry breaking in D-dimensional gauge theories, based on the improved ladder SD equation [18], with the D-dimensional bulk gauge coupling in the ladder SD equation being simply replaced by the [modified minimal subtraction scheme $\overline{MS}$] one-loop running coupling. Actually, in D-dimensional gauge theories for both the fermion and the gauge bosons living in the D-dimensional bulk, with the extra dimensions being compactified, *dynamical symmetry breaking can be triggered only by the dynamics in the ultraviolet region* where the gauge coupling becomes strong, and hence can be well described by the *D-dimensional* improved ladder SD equation, with *massless* gauge bosons *in the D-dimensional bulk*, *irrespectively of details of the infrared dynamics of the compactification scale*.

It is then found that, for the simplest version of the ACDH scenario with only the third family (as well as the gauge bosons) living in the bulk, the UV fixed point of the bulk QCD coupling is smaller than the critical coupling for dynamical chiral symmetry breaking to occur for $D = 6$, while the situation is reversed for $D = 8$. That is *the dynamical symmetry breaking due to the bulk QCD dynamics cannot take place in six dimensions and can in eight dimensions for the simplest ACDH version of the TMSM.*

Remarkably enough, the improved ladder SD equation with *running* coupling has an approximately *scale-invariant form* in D dimensions and thus *the scaling law is the essential-singularity type of "conformal phase transition"* [19] similar to Miransky scaling in the four-dimensional ladder SD equation with *nonrunning* coupling [20]. Moreover, it has a *large anomalous dimension* $\gamma_m = D/2 - 1$ near the fixed point and hence has a chance to solve the flavor-changing-neutral current problem as in walking technicolor for $D = 4$ [21].

This corresponds to a slowly damping mass function that still yields finiteness of the bulk decay constant $F_\pi^{(D)}$ and hence of the induced bulk Yukawa coupling even in the limit of infinite cutoff (in the formal sense). Such a situation is similar to the renormalizability of the gauged NJL model in four dimensions [22].

We also comment that, instead of the $\overline{MS}$ running coupling in the improved ladder SD equation, we may use the "effective" coupling including finite renormalization effects. Unlike $\overline{MS}$ coupling, the "effective" gauge coupling includes the effects of KK modes heavier than the renormalization scale. It is shown that the decoupling theorem is violated in the "effective" gauge coupling due to the summation of the large number of KK modes. Nevertheless, we find an *upper bound* on the effective gauge coupling strength, which is roughly proportional to the UV fixed point in the $\overline{MS}$ scheme. We also show that the upper bound of the "effective" gauge coupling can be regarded as a UV fixed point of "bare gauge coupling." Our results are therefore unchanged qualitatively even if we adopt the "effective" coupling instead of $\overline{MS}$.

It should be emphasized, however, that finite renormalization can affect our quantitative results, such as the value of the critical coupling. The effective coupling tends to be stronger than $\overline{MS}$ coupling and hence there appears the possibility that bulk

SM couplings could lead to the top quark condensate in the manner of Eq. (1.2) under certain conditions even for $D = 6$ in the simplest ACDH version of the TMSM.

The paper is organized as follows. In Section 2 we discuss the existence of the nontrivial UV fixed point in D-[$= (4+\epsilon)$-]-dimensional non-Abelian gauge theories in the ϵ expansion. Then we show the nontrivial UV fixed point in the D-[$= (4+\delta)$-]-dimensional non-Abelian gauge theories with the extra δ $(= 2, 4)$ dimensions compactified. The value of the UV fixed point for the ACDH version of the TMSM is evaluated for $D = 6, 8$ based on the truncated KK effective theory. We then give a rough argument why the "strong" bulk QCD coupling may not necessarily give rise to the condensate, based on a naive dimensional analysis (NDA) [23, 24]. In Section 3 we derive the D-dimensional ladder SD equation, and also the improved ladder SD equation. In Section 4 we find numerically the critical values for DχSB to occur for $D = 6, 8$, which are compared with those of the ACDH couplings estimated in Section 2. The analytical solution is also obtained in further approximation, and shows essential-singular-type scaling. In Section 5 we analyze the operator product expansion (OPE) for the fermion propagator and identify the anomalous dimension, which is then calculated to be $\gamma_m = D/2 - 1$. In Section 6 the chiral fermion through the orbifold projection into the 3-brane is studied in some detail. In Section 7 we discuss use of the effective coupling instead of the $\overline{MS}$ running coupling in the improved ladder SD equation. Section 8 is devoted to the summary and discussion. Appendix A contains formulas for the angular integration of the ladder SD equation, which is a generalization of the previous result [25] to arbitrary (noninteger) D dimensions. Appendix B shows a gap equation of the NJL-type four-fermion model in D (> 4) dimensions, in which the scaling law is $1/g_{crit} - 1/g \sim (m/\Lambda)^2$, essentially the same (up to logarithms) as the NJL model for $D = 4$, in sharp contrast to the case of $D < 4$ where the scaling law is given by $1/g_{crit} - 1/g \sim (m/\Lambda)^{D-2}$ [26]. Appendix C is for the approximation to the effective coupling discussed in Section 7.

2 Existence of ultraviolet fixed point

In order to illustrate the existence of the nontrivial ultraviolet fixed point of the gauge theory in more than four dimensions, we start with a brief review of the gauge dynamics in D $(= 4+\epsilon,\ 0 < \epsilon \ll 1)$ dimensions [27] (ϵ expansion).

The one-loop renormalization-group equation of the gauge coupling is given by

$$\mu \frac{d}{d\mu} \hat{g} = \frac{\epsilon}{2} \hat{g} + \frac{b_{(1)}}{(4\pi)^2} \hat{g}^3, \tag{2.1}$$

where $\hat{g}$ is the dimensionless gauge coupling scaled by a renormalization scale μ:

$$g_D \equiv \frac{\hat{g}}{\mu^{\epsilon/2}}, \tag{2.2}$$

with g_D being the gauge coupling in D $(= 4+\epsilon)$ dimensions and of mass dimension $-\epsilon/2$. Hereafter we assume that the renormalization-group coefficient $b_{(1)}$ is negative, $b_{(1)} < 0$. From Eq. (2.1), the renormalization-group flow of the dimensionless coupling $\hat{g}$ is given by

$$\hat{g}^2(\mu) = \frac{1}{\left(\frac{\mu'}{\mu}\right)^{\epsilon} \frac{1}{\hat{g}^2(\mu')} - \frac{2}{\epsilon}\frac{b_{(1)}}{(4\pi)^2}\left[1 - \left(\frac{\mu'}{\mu}\right)^{\epsilon}\right]}. \tag{2.3}$$

We then find an ultraviolet $(\mu \to \infty)$ fixed point

$$g_*^2 = \lim_{\mu\to\infty} \hat{g}^2(\mu) = \frac{\epsilon}{2}\frac{(4\pi)^2}{-b_{(1)}}. \tag{2.4}$$

It should be emphasized that ϵ is considered to be small here and therefore the fixed point $g_*^2 \propto \epsilon$ is still in its perturbative regime. It is straightforward to extend the analysis to include higher-loop effects. The UV fixed point in the two-loop RGE,

$$\mu\frac{d}{d\mu}\hat{g} = \frac{\epsilon}{2}\hat{g} + \frac{b_{(1)}}{(4\pi)^2}\hat{g}^3 + \frac{b_{(2)}}{(4\pi)^4}\hat{g}^5 \tag{2.5}$$

is given in terms of the ϵ expansion,

$$g_*^2 = \frac{(4\pi)^2}{-b_{(1)}}\frac{\epsilon}{2}\left(1 + \frac{b_{(2)}}{b_{(1)}^2}\frac{\epsilon}{2}\right) + \mathcal{O}(\epsilon^3). \tag{2.6}$$

The two-loop effect, $b_{(2)}$ term affects the coefficient of ϵ^2, keeping the coefficient of ϵ^1 unchanged. In fact, the n-loop effect can be regarded as an $\mathcal{O}(\epsilon^n)$ effect in the ϵ expansion. The perturbative stability of the fixed point g_* is thus guaranteed in the D-[$= (4+\epsilon)$-]-dimensional gauge theories. We also note that the coefficients $b_{(1)}$ and $b_{(2)}$ are both negative in QCD with $N_f \leq 8$. The two-loop UV fixed point Eq. (2.6) is thus smaller than the one-loop estimate Eq. (2.4).

Hence we expect that there exist (at least) two phases separated by the fixed point g_* in this theory. The weakly interacting phase $\hat{g} < g_*$ can be controlled perturbatively. It is therefore considered to be in the Coulomb phase and the chiral symmetry is not broken in this phase. On the other hand, the theory becomes strongly interacting in the low-energy region in the phase $\hat{g} > g_*$. It is therefore expected to be in the confinement phase and the chiral symmetry is expected to be broken dynamically.

Although the existence of such a fixed point for larger $\epsilon \sim \mathcal{O}(1)$ cannot be justified within perturbative analysis, recent analysis based on the lattice gauge theory [28] suggests that the fixed point structure described above holds even at larger (integer) values of ϵ, if the extra dimensions are compactified in a short distance.[2] Actually, as

[2] There still exists nontrivial phase structure even in the case of noncompactified extra dimensions. However, the phase transition is shown to be first order [29] and we cannot obtain hierarchy between the cutoff scale and the low-energy scales.

we will see in the following, there exists a close correspondence between the RGEs of $\epsilon \ll 1$ and of the compactified extra dimensions even within the perturbative approach.

Now we evaluate the *nontrivial UV fixed point of the gauge theory in* D $(= 4 + \delta)$ *dimensions where the extra* δ *dimensions are compactified.* In this case we need to deal with an infinite number of KK modes above the compactification scale R^{-1}. However, the KK modes heavier than the renormalization scale μ are actually decoupled in the RGE. We only need to sum up the loops of KK modes lighter than μ. This approach is called "truncated KK" effective theory [17]. The theory can be fully controlled in this truncated KK effective theory.

The RGE of the gauge coupling (g) on the 3-brane is given by

$$(4\pi)^2 \mu \frac{d}{d\mu} g = N_{\rm KK} b' g^3 \tag{2.7}$$

in the truncated KK effective theory. Here $N_{\rm KK}$ stands for the number of KK modes below the renormalization scale μ. The RGE factor b' is given by

$$b' = -\frac{26 - D}{6} C_G + \frac{\eta}{3} T_R N_f, \tag{2.8}$$

where η represents the dimension of the spinor representation of $SO(1, D-1)$,

$$\eta \equiv {\rm tr}_\Gamma 1 = 2^{D/2} \qquad \text{for even } D, \tag{2.9}$$

and N_f is the number of fermions in the bulk. The group-theoretical factors C_G and T_R are given by $C_G = N$ and $T_R = 1/2$ for $SU(N)$ gauge theory.

For sufficiently large $\mu \gg R^{-1}$, $N_{\rm KK}$ is estimated as [17]

$$N_{\rm KK} = \frac{1}{n} \frac{\pi^{\delta/2}}{\Gamma(1 + \delta/2)} (\mu R)^\delta, \tag{2.10}$$

where we have assumed that the extra dimensions are compactified to an orbifold T^δ/Z_n with Z_n being a discrete group with order of n.

The gauge coupling on the 3-brane can be related to the gauge coupling in the D-dimensional bulk g_D as $g_D^2 = (2\pi R)^\delta g^2/n$. Thus the *dimensionless* bulk gauge coupling $\hat{g}$ can be defined following Eq. (2.2):

$$\hat{g}^2 = \frac{(2\pi R\mu)^\delta}{n} g^2. \tag{2.11}$$

Substituting Eq. (2.11) into Eq. (2.7), we obtain

$$\mu \frac{d}{d\mu} \hat{g} = \frac{\delta}{2} \hat{g} + (1 + \delta/2) \Omega_{\rm NDA} b' \hat{g}^3, \tag{2.12}$$

with $\Omega_{\rm NDA}$ being the loop factor in the NDA [23, 24]:

$$\Omega_{\rm NDA} \equiv \frac{1}{(4\pi)^{D/2}\Gamma(D/2)}, \qquad D = 4+\delta. \tag{2.13}$$

It is interesting to note a similarity between Eq. (2.1) and Eq. (2.12): The factor ϵ in the ϵ expansion corresponds to δ in the truncated KK effective theory with the simple replacement of $b/(4\pi)^2$ by $(1+\delta/2)\Omega_{\rm NDA} b'$.

The RGE Eq. (2.12) can easily be solved as

$$\hat{g}^2(\mu) = \frac{1}{\left(\frac{\mu'}{\mu}\right)^{\delta} \frac{1}{\hat{g}^2(\mu')} - \left(\frac{2}{\delta}+1\right)\Omega_{\rm NDA} b' \left[1 - \left(\frac{\mu'}{\mu}\right)^{\delta}\right]}. \tag{2.14}$$

Thus, we find a *nontrivial UV fixed point*

$$g_*^2 \Omega_{\rm NDA} = \frac{1}{-\left(\frac{2}{\delta}+1\right) b'}. \tag{2.15}$$

It should be noted that the coupling $\hat{g}^2$ in Eq. (2.14) grows very quickly close to the value of the fixed point.

In the ACDH scenario [7] of the TMSM, the top quark interaction responsible for the dynamical electroweak symmetry breaking is assumed to come (mainly) from the bulk QCD interaction. On the other hand, the low-energy QCD coupling in the 3-brane is obviously well below its fixed point. [$\hat{g}^2/g_*^2 \simeq 1.83\alpha/n$ ($0.72\alpha/n$) with $\alpha \equiv g^2/(4\pi)$ for $D=6$ ($D=8$) at $\mu = R^{-1}$.] Thus, Eq. (2.15) can be regarded as *the upper bound of the dimensionless coupling of the bulk QCD*. In fact, in the ACDH scenario for $D=6$ the upper bound of the dimensionless QCD coupling is given by

$$C_F \hat{g}^2 \Omega_{\rm NDA} < C_F g_*^2 \Omega_{\rm NDA} \simeq 0.09, \tag{2.16}$$

where we have used $\delta = 2$, $\eta = 8$, $C_F = 4/3$, $C_G = 3$, and $N_f = 2$ in Eqs. (2.8) and (2.15). Even though the value of g_* can be affected by the higher-loop effects, it is proportional to $1/(-b')$ for sufficiently large $-b'$.[3] Equation (2.16) implies that, although the bulk QCD coupling is generally expected to become "strong" in the region beyond the compactification scale, it is actually *not so strong* as to make the perturbative expansion totally useless. Moreover, an analysis similar to Eq. (2.6) indicates that the value of g_* of the bulk QCD with $\delta = 2$ and $N_f = 2$ tends to be decreased by taking

[3] It should be emphasized, however, that the higher-loop effects cannot be made arbitrarily small even in the large $-b'$ (>0) limit. Equation (2.8) shows that large $-b'$ corresponds to large C_G (and small N_f) with $C_G = N$ for $SU(N)$ gauge theory. The typical size of the n-loop effect at the fixed point is thus of order $(N g_*^2 \Omega_{\rm NDA})^n \sim [N/(-b')]^n \simeq [6/(26-D)]^n$ even in the large N limit.

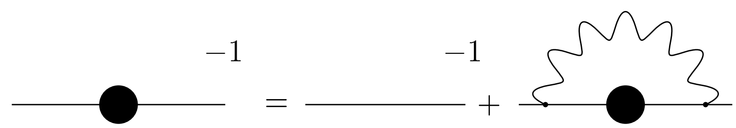

Figure 1: Feynman diagram of the SD equation in the ladder approximation. Solid lines with and without a blob represent dressed and bare propagators of fermions [$S(p)$, $S_0(p)$], respectively. The gauge boson-propagator (D_{MN}) is denoted by a wavy line.

into account the two-loop effects. The estimate Eq. (2.16) can thus be regarded as a conservative one, although we expect sizable higher-loop uncertainty in our estimate.

It is therefore quite *nontrivial whether bulk QCD can be strong enough to trigger dynamical electroweak symmetry breaking*. Before starting a detailed analysis, it would be helpful to give a simpler discussion from the viewpoint of the NDA [23, 24] and MAC [16], which leads to the condition for the dynamical symmetry breaking to take place

$$C_F \hat{g}^2 \Omega_{\rm NDA} \gtrsim 1, \tag{2.17}$$

where $\Omega_{\rm NDA}$ comes from the loop suppression factor of NDA and C_F is the quadratic Casimir of the fundamental representation, which is from the MAC assumption. Hence Eq. (2.16) suggests that bulk QCD may not be enough to induce dynamical electroweak symmetry breaking in the ACDH scenario in six dimensions.

However, the present analysis might be too simple minded. In the following sections we will investigate this issue using the SD gap equation within the improved ladder approximation.

3 Improved ladder Schwinger-Dyson equation

3.1 Ladder SD equation

We next investigate the condition for the chiral symmetry to break dynamically in gauge theories in dimensions $D > 4$. The dimensions of the space-time D need to be even in order that the chiral symmetry is defined in the bulk. Since the electroweak symmetry is a chiral symmetry, the condition studied in this section can be regarded as the condition for dynamical electroweak symmetry breaking in the bulk.

Bulk DχSB in gauge theories with extra dimensions is considered as a nonperturbative effect of the high-energy region [7] where the SM gauge couplings in the D-dimensional bulk become strong. We therefore neglect the infrared dynamics due to the finite size effects of extra dimensions in the following.

The D-dimensional ladder SD equation for the fermion propagator is given by Fig. 1.

It then reads

$$iS^{-1}(p) = iS_0^{-1}(p) + \int \frac{d^D q}{(2\pi)^D i} \left[-ig_D T^a \Gamma^M\right] S(q) \left[-ig_D T^a \Gamma^N\right] D_{MN}(p-q), \tag{3.1}$$

where S and S_0 denote dressed and bare propagators of the fermion, respectively. Within the ladder approximation, the gauge boson propagator D_{MN} is approximated at the tree level by the form

$$D_{MN}(p-q) = \frac{-i}{(p-q)^2}\left[g_{MN} - (1-\xi)\frac{(p-q)_M (p-q)_N}{(p-q)^2}\right], \tag{3.2}$$

with ξ being a gauge-fixing parameter. We also indicate the the gamma matrix of $SO(1, D-1)$ by Γ^M

$$\{\Gamma^M, \Gamma^N\} = 2g^{MN}, \qquad M, N = 0, 1, 2, 3, 5, \cdots, D. \tag{3.3}$$

Since we are dealing with DχSB in the bulk, we take the bare propagator of the fermion in D dimensions to be massless, $iS_0^{-1}(p) = \not{p}$. The dressed propagator S may be written as

$$iS^{-1}(p) = A(-p^2)\not{p} - B(-p^2). \tag{3.4}$$

Then Eq. (3.1) leads to coupled SD equations after Wick rotation:

$$\begin{aligned} A(p_E^2) &= 1 + \frac{C_F g_D^2}{p_E^2} \int \frac{d^D q_E}{(2\pi)^D} \frac{A(q_E^2)}{A^2 q_E^2 + B^2} \\ &\times \left[-(3-D-\xi)\frac{p_E \cdot q_E}{(p_E - q_E)^2} + 2(1-\xi)\frac{p_E \cdot (p_E - q_E) q_E \cdot (p_E - q_E)}{(p_E - q_E)^4}\right], \end{aligned} \tag{3.5}$$

$$B(p_E^2) = (D - 1 + \xi) C_F g_D^2 \int \frac{d^D q_E}{(2\pi)^D} \frac{B(q_E^2)}{A^2 q_E^2 + B^2} \frac{1}{(p_E - q_E)^2}, \tag{3.6}$$

where p_E and q_E denote the Euclidean momenta $p_E^2 \equiv -p^2$, $q_E^2 \equiv -q^2$, respectively. Performing the angular integrals in Eq. (3.5) and Eq. (3.6), we find

$$A(x) = 1 + 2\frac{D-2}{D}\xi \Omega_{\rm NDA} \frac{C_F}{x} \int_0^{\Lambda^2} dy y^{D/2-1} \frac{g_D^2 A(y)}{A^2 y + B^2} K_A(x, y), \tag{3.7}$$

$$B(x) = (D - 1 + \xi)\Omega_{\rm NDA} C_F \int_0^{\Lambda^2} dy y^{D/2-1} \frac{g_D^2 B(y)}{A^2 y + B^2} K_B(x, y), \tag{3.8}$$

with $x \equiv p_E^2$, $y \equiv q_E^2$, where we have introduced the ultraviolet cutoff Λ, which is believed to have physical meaning such as the string scale in this class of models with extra dimensions.

The integral kernels K_A and K_B are given in Ref. [25] and are explicitly written as

$$K_A(x,y) = \frac{y}{x}\theta(x-y) + (x \leftrightarrow y), \tag{3.9}$$

$$K_B(x,y) = \frac{1}{x}\theta(x-y) + (x \leftrightarrow y) \tag{3.10}$$

for $D = 4$,

$$K_A(x,y) = \frac{y}{x}\left(1 - \frac{y}{2x}\right)\theta(x-y) + (x \leftrightarrow y), \tag{3.11}$$

$$K_B(x,y) = \frac{1}{x}\left(1 - \frac{y}{3x}\right)\theta(x-y) + (x \leftrightarrow y) \tag{3.12}$$

for $D = 6$, and

$$K_A(x,y) = \frac{y}{x}\left(1 - \frac{4y}{5x} + \frac{y^2}{5x^2}\right)\theta(x-y) + (x \leftrightarrow y), \tag{3.13}$$

$$K_B(x,y) = \frac{1}{x}\left(1 - \frac{y}{2x} + \frac{y^2}{10x^2}\right)\theta(x-y) + (x \leftrightarrow y) \tag{3.14}$$

for $D = 8$. (See Appendix A for details.)

Hereafter, we will use the Landau gauge $\xi = 0$ in which the wave function renormalization is absent $[A(x) \equiv 1]$ within the ladder approximation.

3.2 Improved ladder SD equation

It should be recalled here that we have so far neglected effects of the running of the gauge coupling. The powerlike behavior of the running coupling makes its effects extremely important, however. In the analysis of DχSB in four-dimensional gauge theories, a widely used approximation is the so-called "improved" ladder approximation [18], in which the renormalization point μ^2 of the running coupling constant in the SD equation is replaced by $\max(p_E^2, q_E^2)$. This is a successful approximation for explaining properties of low energy QCD phenomenology. In the following analysis we adopt the improved ladder approximation and replace the gauge coupling g_D^2 in Eq. (3.8) by

$$g_D^2 \to g_D^2(p_E, q_E) = \frac{\hat{g}^2(|p_E|)}{(p_E^2)^{\delta/2}}\theta(|p_E| - |q_E|) + \frac{\hat{g}^2(|q_E|)}{(q_E^2)^{\delta/2}}\theta(|q_E| - |p_E|). \tag{3.15}$$

As we discussed in Section 2, the UV fixed point g_* plays the role of the upper bound of $\hat{g}$ in the ACDH scenario of the TMSM. We also note that the *dimensionless* bulk gauge coupling $\hat{g}$ in Eq. (2.14) approaches its fixed point very quickly for $\mu > 1/R$ due to its power-law running and hence is *near the fixed point value over a wide range of*

the momentum in the integral of the SD equation. For determination of the condition of the bulk DχSB, it is therefore sufficient to investigate the SD equation with the coupling just on the UV fixed point:

$$B(x) = (D-1)\kappa_D \int_{M_0^2}^{\Lambda^2} dy y^{D/2-1} \frac{B(y)}{y + B^2(y)} K_B^{\rm imp}(x,y) \tag{3.16}$$

with

$$\kappa_D \equiv C_F g_*^2 \Omega_{\rm NDA} = \frac{C_F}{\left(\dfrac{2}{D-4}+1\right)\left[\dfrac{26-D}{6}C_G - \dfrac{\eta}{3}T_R N_f\right]}, \tag{3.17}$$

where we have used Eqs. (2.8) and (2.15), and $K_B^{\rm imp}$ is given by

$$K_B^{\rm imp}(x,y) = \frac{1}{x^2}\left(1 - \frac{y}{3x}\right)\theta(x-y) + (x \leftrightarrow y) \qquad \text{for } D = 6 \tag{3.18}$$

and

$$K_B^{\rm imp}(x,y) = \frac{1}{x^3}\left(1 - \frac{y}{2x} + \frac{y^2}{10x^2}\right)\theta(x-y) + (x \leftrightarrow y) \qquad \text{for } D = 8. \tag{3.19}$$

Since the extra dimensions are compactified below the scale $1/R$, we have introduced the infrared (IR) cutoff M_0 in Eq. (3.16). However, *the bulk DχSB becomes insensitive to M_0 for large Λ* as we will show in the next section. It is to be noted that the resulting *improved ladder* SD equation with *running* coupling in Eq. (3.16) is a *scale-invariant* form, similar to the ladder SD equation with *constant* gauge coupling in four dimensions.

We note that, in the improved ladder SD equation Eq. (3.16), the κ_D defined by Eq. (3.17) plays the role of a "coupling." It can be shown that there exists a critical κ_D above which DχSB takes place for sufficiently large Λ in the bulk.

4 Analysis of the improved ladder SD equation

4.1 Numerical study

The aim of this section is to determine the critical κ_D (and the scaling behavior around $\kappa_D^{\rm crit}$) by solving the SD equation Eq. (3.16) in a numerical method.

Let us start with the case $D = 6$ and consider a discretized version of Eq. (3.16):

$$B_i = 5\kappa_6 \left[\sum_{j=1}^{i} \frac{x_j B_j}{x_j + B_j^2}\frac{x_j^2}{x_i^2}\left(1 - \frac{x_j}{3x_i}\right) + \sum_{j=i+1}^{i_\Lambda} \frac{x_j B_j}{x_j + B_j^2}\left(1 - \frac{x_i}{3x_j}\right)\right] \tag{4.1}$$

with i, j being integer indices and

$$x_j \equiv M_0^2 \exp\left[\frac{j-1}{i_\Lambda - 1}\ln\frac{\Lambda^2}{M_0^2}\right], \qquad B_j \equiv B(x_j). \tag{4.2}$$

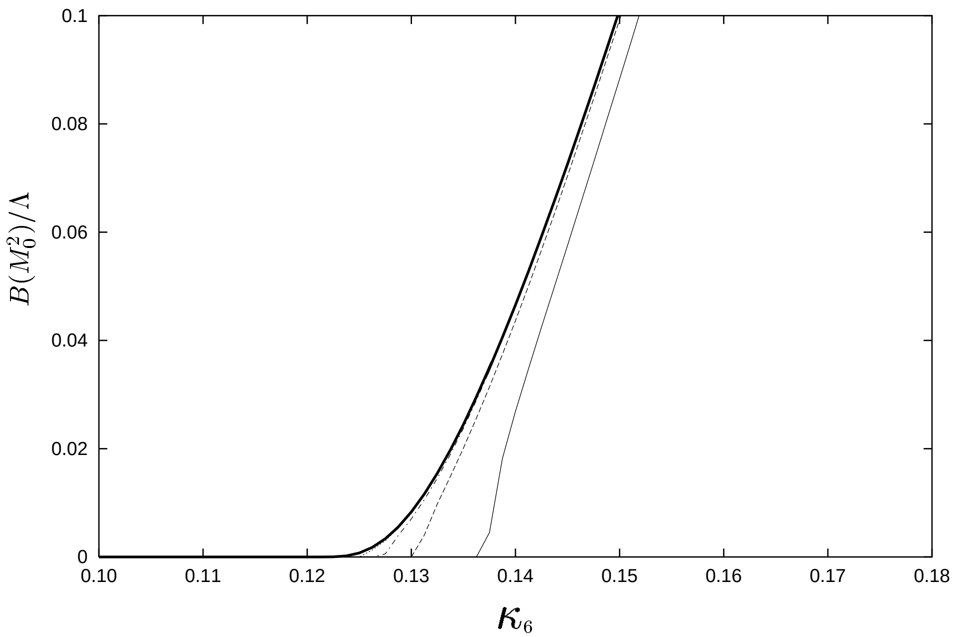

Figure 2: The scaling behavior in six dimensions. The lines from right to left are graphs for $\Lambda^2/M_0^2 = 10^3, 10^4, 10^5, 10^6, 10^{10}$, respectively.

In order to solve the discretized SD equation Eq.(4.1), a series $B_j^{(n)}$ is defined by a recursion relation,

$$B_i^{(n+1)} \equiv 5\kappa_6 \left[\sum_{j=1}^{i} \frac{x_j B_j^{(n)}}{x_j + (B_j^{(n)})^2} \frac{x_j^2}{x_i^2} \left(1 - \frac{x_j}{3x_i}\right) + \sum_{j=i+1}^{i_\Lambda} \frac{x_j B_j^{(n)}}{x_j + (B_j^{(n)})^2} \left(1 - \frac{x_i}{3x_j}\right) \right] \quad (4.3)$$

and the initial condition

$$B_j^{(n=0)} = M_0 \qquad \text{for } j = 1, 2, \ldots, i_\Lambda. \quad (4.4)$$

For sufficiently large n, the series $B_j^{(n)}$ is numerically shown to converge to a certain B_j, which is nothing but the solution of the SD equation Eq.(4.1). It is also confirmed that the solution is insensitive to the value of i_Λ, if i_Λ is taken to be large enough.

Figure 2 shows the scaling behavior of the order parameter of DχSB, $B(M_0) = B_{j=1}$, near the critical κ_6. We find

$$\kappa_6^{\mathrm{crit}} \simeq 0.122. \quad (4.5)$$

On the other hand, the κ_6 of the ACDH scenario with $D = 6$ (QCD with two flavor fermions in the bulk) can be calculated from Eq. (3.17). We find

$$\kappa_6^{\mathrm{ACDH}} = \frac{1}{11} \simeq 0.091, \quad (4.6)$$

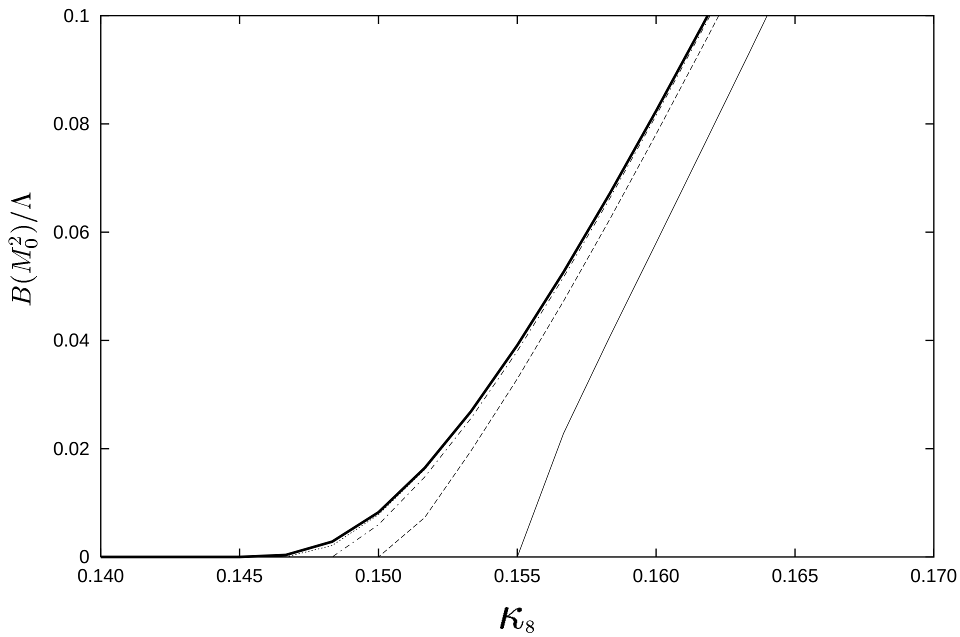

Figure 3: The scaling behavior in eight dimensions. The lines from right to left are graphs for $\Lambda^2/M_0^2 = 10^3, 10^4, 10^5, 10^6, 10^{10}$, respectively.

where we have used $C_F = 4/3$, $C_G = 3$, $N_f = 2$, and $\eta = 8$. Note that this is the *upper bound* of the bulk QCD coupling. We therefore conclude that the simplest version of the ACDH scenario does not work properly in $D = 6$ dimensions within the improved ladder approximation.

A similar analysis is also performed for $D = 8$ dimensions. We obtain the scaling behavior of Fig. 3, and the critical κ_8

$$\kappa_8^{\rm crit} \simeq 0.146. \tag{4.7}$$

Since the ACDH scenario in $D = 8$ dimensions predicts

$$\kappa_8^{\rm ACDH} = \frac{8}{33} \simeq 0.242, \tag{4.8}$$

there is the possibility to construct viable models in $D = 8$ within the improved ladder approximation.

One may doubt the validity of the ladder approximation in this model. The size of nonladder corrections is estimated to be 1%–20% in the analysis of four-dimensional walking technicolor [30]. We expect a similar size of nonladder corrections in the present model. On the other hand, the fixed point Eq. (4.6) is smaller than the critical value Eq. (4.5) by more than 25%. Although it is extremely difficult to draw a definite conclusion from these numbers, it is likely that the ACDH scenario in $D = 6$ dimensions is still in the chiral symmetric phase even in beyond-the-ladder approximations. We

also note that the ladder results are qualitatively consistent with the naive dimensional analysis described in Section 2. The bulk QCD coupling is not so strong as to destroy the perturbative picture completely, anyway. We thus expect that our results (Fig. 2 and Fig. 3) will be unchanged qualitatively even beyond the ladder approximation.

4.2 Analytical study

The improved ladder SD equation can be investigated analytically by applying further approximations. The SD equation can be greatly simplified if the integral kernel $K_B^{\rm imp}$ is approximated by

$$\tilde{K}_B^{\rm imp}(x,y) = \frac{1}{x^{D/2-1}}\theta(x-y) + (x \leftrightarrow y). \tag{4.9}$$

The approximation Eq. (4.9) can be justified in a wide range of the integral region ($x \not\simeq y$) in Eq. (3.16). We also note that the kernel Eq. (4.9) has scale invariance like the original kernel $K_B^{\rm imp}$.

Although the SD equation Eq. (3.16) is still nonlinear even under this approximation, we can overcome the difficulty by using the bifurcation technique [31], in which the mass function B in the denominator in the SD equation is eliminated and an infrared cutoff $M \equiv B(M^2)$ is introduced instead. The bifurcation technique is justified when κ_D is close to its critical point.

The SD equation Eq. (3.16) then leads to a linear equation

$$B(x) = (D-1)\kappa_D \int_{M^2}^{\Lambda^2} dy y^{D/2-2} B(y) \tilde{K}_B^{\rm imp}(x,y) \tag{4.10}$$

and a subsidiary condition

$$M = B(M^2). \tag{4.11}$$

The integral equation Eq. (4.10) is equivalent to a set of a differential equation,

$$\left[x^2 \frac{d^2}{dx^2} + \frac{D}{2} x \frac{d}{dx} + (D-1)(D/2-1)\kappa_D\right] B(x) = 0, \tag{4.12}$$

and boundary conditions

$$\frac{d}{dx} B(x)\bigg|_{x=M^2} = 0 \qquad \text{(IR-BC)} \tag{4.13}$$

$$\left[x\frac{d}{dx} - 2\omega\right] B(x)\bigg|_{x=\Lambda^2} = 0 \qquad \text{(UV-BC)}, \tag{4.14}$$

with ω being defined by

$$\omega \equiv -\frac{1}{2}\left(\frac{D}{2} - 1\right). \tag{4.15}$$

It is easy to solve the differential equation Eq. (4.12). Combined with the subsidiary condition Eq. (4.11) and the infrared boundary condition (IR-BC), we find

$$\frac{B(x)}{M} = \frac{1}{2\tilde{\nu}} \left(\frac{x}{M^2}\right)^{\omega} \left[(1+\tilde{\nu})\left(\frac{x}{M^2}\right)^{-\omega\tilde{\nu}} - (1-\tilde{\nu})\left(\frac{x}{M^2}\right)^{\omega\tilde{\nu}}\right], \quad \tilde{\nu} \equiv \sqrt{1-\kappa_D/\kappa_D^{\mathrm{crit}}}, \tag{4.16}$$

for $\kappa_D < \kappa_D^{\mathrm{crit}}$ and

$$\frac{B(x)}{M} = \frac{1}{2i\nu} \left(\frac{x}{M^2}\right)^{\omega} \left[(1+i\nu)\left(\frac{x}{M^2}\right)^{-i\omega\nu} - (1-i\nu)\left(\frac{x}{M^2}\right)^{i\omega\nu}\right], \quad \nu \equiv \sqrt{\kappa_D/\kappa_D^{\mathrm{crit}}-1}, \tag{4.17}$$

for $\kappa_D > \kappa_D^{\mathrm{crit}}$, where we find the critical κ_D

$$\kappa_D^{\mathrm{crit}} \equiv \frac{1}{8}\frac{D-2}{D-1}. \tag{4.18}$$

Actually, the nonoscillating solution Eq. (4.16) for $\kappa_D < \kappa_D^{\mathrm{crit}}$ does not satisfy the ultraviolet boundary condition (UV-BC). A nontrivial solution of Eq. (4.10) exists only for $\kappa_D > \kappa_D^{\mathrm{crit}}$, where the solution Eq. (4.17) starts oscillating. The critical κ_D Eq. (4.18) reads $\kappa_6^{\mathrm{crit}} = 1/10$ and $\kappa_8^{\mathrm{crit}} = 3/28$, which are slightly smaller than the numerical results in the previous section, Eq. (4.5) and Eq. (4.7). Noting the inequality of the integral kernels $K_B^{\mathrm{imp}} < \tilde{K}_B^{\mathrm{imp}}$, however, these results are consistent with each other.

We next turn to the scaling behavior near the critical point. Equation (4.17) can be rewritten as

$$\frac{B(x)}{M} = \frac{\sqrt{1+\nu^2}}{\nu}\left(\frac{x}{M^2}\right)^{\omega} \sin\left[\theta - \omega\nu\ln\frac{x}{M^2}\right], \qquad e^{i\theta} \equiv \frac{1+i\nu}{\sqrt{1+\nu^2}}. \tag{4.19}$$

Inserting Eq. (4.19) into the UV-BC Eq. (4.14), we obtain

$$\theta - \omega\nu\ln\frac{\Lambda^2}{M^2} + \tan^{-1}\nu = n\pi, \tag{4.20}$$

with n being a positive integer. It can be shown that the ground state corresponds to the zero-node ($n=1$) solution [32]. Noting that $\theta = \tan^{-1}\nu \simeq \nu$ for $\nu \ll 1$, we thus obtain the scaling relation near the critical point,

$$M \propto \Lambda \exp\left[\frac{-\pi}{(D/2-1)\sqrt{\kappa_D/\kappa_D^{\mathrm{crit}}-1}}\right]. \tag{4.21}$$

Thus we found that the scaling of the phase transition Eq. (4.21) is an essential-singularity type, the "conformal phase transition" [19], similar to the result of the

quenched ladder SD equation of four-dimensional QED [20]. It is suggestive that, as we noted at the end of Section 3, these SD equations are both scale invariant.

It is also worth pointing out that the essential singularity may be used to construct models with large hierarchy between the cutoff and the weak scale without introducing additional fine tuning. This important property of our analysis is contrasted with the NJL approach [7], where we need fine tuning of the NJL coupling strength with the $(M/\Lambda)^2$ level. (See Appendix B for details.)

Near the critical point ($\nu \to 0$ limit), Eq. (4.19) gives

$$B(x) = M\left(\frac{x}{M^2}\right)^{-(D/2-1)/2}\left(1+\frac{1}{2}\left(\frac{D}{2}-1\right)\ln\frac{x}{M^2}\right), \tag{4.22}$$

which is regarded as the asymptotic behavior of the solution of the SD equation Eq. (3.16).

5 Anomalous dimension of the fermion mass

We next consider generally the high-energy behavior of the dynamical mass when DχSB takes place, based on the OPE [33].

The OPE of the time-ordered fermion bilinear operator $T[\psi(x)\bar{\psi}(0)]$ is given by

$$-i\int d^D x e^{iq\cdot x} T[\psi_i^a(x)\bar{\psi}_b^j(0)] = c_1^M(q, g_D;\mu)(\Gamma_M)_i{}^j\delta^a{}_b + c_{\bar{\psi}\psi}(q, g_D;\mu)\delta_i{}^j\delta^a{}_b(\bar{\psi}\psi) + \cdots, \tag{5.1}$$

with c_1, $c_{\bar{\psi}\psi}$ being the Wilson coefficient functions, where a, b are for gauge indices and i, j are for spinor indices.

It is straightforward to evaluate the Wilson coefficient function $c_{\bar{\psi}\psi}$ in the D-[$=(4+\delta)$-]-dimensional gauge theories at the tree level,

$$c_{\bar{\psi}\psi}(q, \hat{g};\mu) = \frac{(D-1)}{\eta}\frac{C_F}{N}\frac{\hat{g}^2}{\mu^\delta}\frac{1}{q^4}, \tag{5.2}$$

where we adopted the Landau gauge. Comparing Eq. (5.1) with the propagator of the fermion field

$$-iS(p) = \frac{1}{A(-p^2)\not{p} - B(-p^2)} \simeq \frac{\not{p}}{A(-p^2)p^2} + \frac{B(-p^2)}{A^2(-p^2)p^2} + \cdots, \tag{5.3}$$

we find that the high-energy behavior of the dynamical fermion mass function $B(-p^2)$ is given by

$$B(-p^2) \simeq p^2 c_{\bar{\psi}\psi}(p, \hat{g};\mu)\langle\bar{\psi}\psi\rangle, \tag{5.4}$$

where we have assumed absence of wave-function renormalization of the fermion field, which is justified in the Landau gauge within the ladder approximation.

The solution of the RGE for $c_{\bar{\psi}\psi}$ is given by,

$$\left[\frac{\partial}{\partial t} - \hat{\beta}\frac{\partial}{\partial \hat{g}} + D - \gamma_m(\hat{g})\right] c_{\bar{\psi}\psi}(e^t p, \hat{g}; \mu) = 0, \tag{5.5}$$

which is solved as

$$c_{\bar{\psi}\psi}(e^t p, \hat{g}; \mu) = c_{\bar{\psi}\psi}(p, \bar{g}(t); \mu) \exp \int_0^t dt \left[\gamma_m(\bar{g}(t)) - D\right], \tag{5.6}$$

with the running gauge coupling $\bar{g}(t)$:

$$\bar{g}^2(t) = \frac{1}{\dfrac{e^{-\delta t}}{\hat{g}^2(\mu)} - \left(\dfrac{2}{\delta} + 1\right) \Omega_{\rm NDA} b \left[1 - e^{-\delta t}\right]}. \tag{5.7}$$

For sufficiently large t, it is evident that $\lim_{t\to\infty} \bar{g}(t) = g_*$. The high-energy behavior of the Wilson coefficient function $c_{\bar{\psi}\psi}$ therefore reads

$$c_{\bar{\psi}\psi}(e^t p, \hat{g}; \mu) \propto e^{(\gamma_m^* - D)t}, \qquad \gamma_m^* \equiv \gamma_m(g_*), \tag{5.8}$$

or

$$c_{\bar{\psi}\psi}(p, \hat{g}; \mu) \propto (-p^2)^{(\gamma_m^* - D)/2}. \tag{5.9}$$

The high-energy behavior of the mass function B in Eq. (5.4) thus is given by

$$B(-p^2) \propto (-p^2)^{(\gamma_m^* + 2 - D)/2}. \tag{5.10}$$

The anomalous dimension at the fixed point γ_m^* can be extracted from the numerical solution of the SD equation. For this purpose we define the "power" of the mass function (ω)

$$\omega \equiv \frac{x}{B(x)} \frac{d}{dx} B(x). \tag{5.11}$$

Figure 4 shows the "power" behaviors of the numerical solution of the SD equation in six dimensions for various "couplings." It can be seen that the "power" is almost constant in the asymptotic region $B^2(M_0) \ll x \ll \Lambda^2$ as we expected from Eq. (5.10). The behavior near the cutoff $x \simeq \Lambda^2$ in Fig. 4 is an artifact [34] due to the sharp cutoff introduced in the analysis of the SD equation.[4] This artifact disappears at the limit of $\Lambda \to \infty$. Reading the "power" in the asymptotic region ($\omega \simeq -1$), we obtain

$$\gamma_m^* \simeq 2\omega + (D - 2) \simeq 2 \tag{5.12}$$

for the $D = 6$ bulk gauge theory at the critical point $\kappa_6^{\rm crit}$.

[4] Equation (4.14) leads to the relation of $\Lambda^2 B'(\Lambda^2)/B(\Lambda^2) = 1 - D/2$.

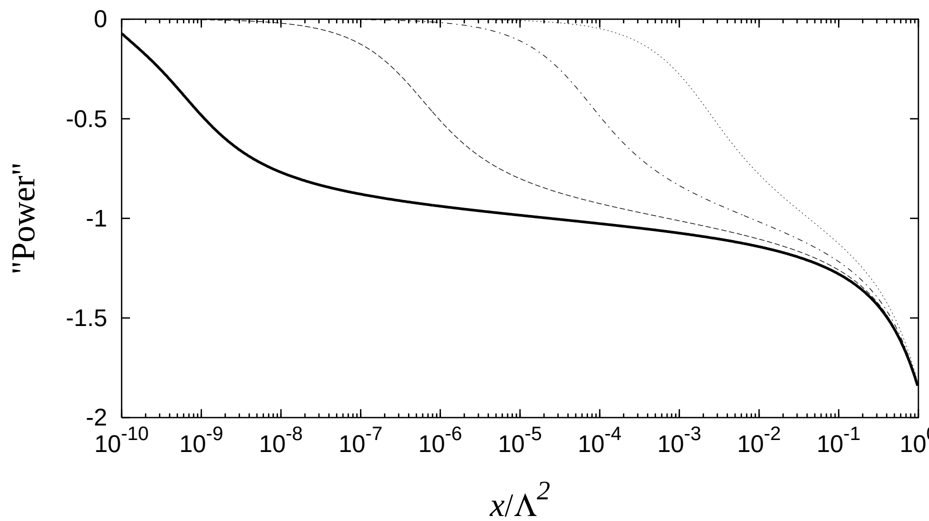

Figure 4: The "power" behavior of the mass function in six dimensions. The lines from left to right represent graphs for $\kappa_6 = 0.122, 0.125, 0.130, 0.140$ [or $B^2(M_0^2)/\Lambda^2 = 4.1 \times 10^{-10}, 5.4 \times 10^{-7}, 6.9 \times 10^{-5}, 2.2 \times 10^{-3}$] with $\Lambda^2/M_0^2 = 10^{10}$.

A similar analysis is also performed for $D = 8$. The corresponding "power" behavior is shown in Fig. 5. The anomalous dimension is then

$$\gamma_m^* \simeq 2\omega + (D-2) \simeq 3, \tag{5.13}$$

for $D = 8$.

The analytical result in the previous section Eq. (4.22) compared with Eq. (5.10) yields

$$\gamma_m^* = \frac{D}{2} - 1, \tag{5.14}$$

which agrees with the above numerical result.

It is remarkable that Eq. (5.14) is also consistent with the conformal phase transitions for other dimensions $D \leq 4$: $\gamma_m = 1/2$ for $D = 3$ agrees with the high-energy behavior [35] and $\gamma_m = 1$ for $D = 4$ is the walking theory [21] obtained from the ladder SD equation with fixed coupling. They are obtained in different approximations: Namely, the result for three dimensions is obtained by running coupling with the IR fixed point and that for six/eight dimensions by running coupling with the UV fixed point, while the four-dimensional result is obtained by fixed coupling. However, the SD equations in all these cases happen to be quite similar because of the *scale invariance at the fixed point*.

It should be emphasized that such a large anomalous dimension implies suppression of the flavor-changing-neutral-current problem in the dynamical electroweak symmetry breaking scenario as in walking technicolor [21]. The large γ_m observed in this section

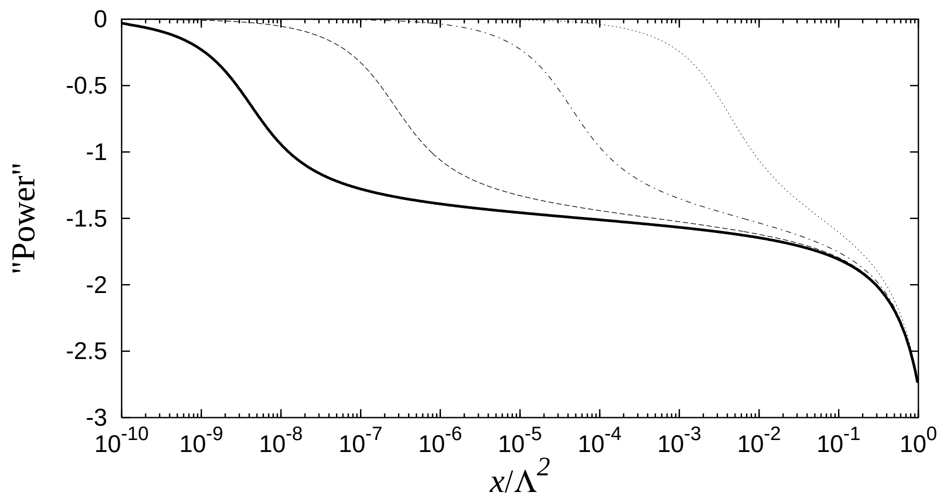

Figure 5: The "power" behavior of the mass function in eight dimensions. The lines from left to right represent graphs for $\kappa_8 = 0.146, 0.147, 0.150, 0.160$ [or $B^2(M_0^2)/\Lambda^2 = 5.8 \times 10^{-9}, 4.1 \times 10^{-7}, 6.8 \times 10^{-5}, 6.8 \times 10^{-3}$] with $\Lambda^2/M_0^2 = 10^{10}$.

is, therefore, good news for constructing phenomenologically viable models in this direction.

Moreover, the corresponding asymptotic behavior of the mass function Eq. (4.22), $B(p_E^2) \sim M^{D/2}(p_E^2)^{(1-D/2)/2}$, still yields strong convergence of the bulk decay constant $F_\pi^{(D)}$, which may be calculated through the PS formula [4]:

$$\begin{aligned} (F_\pi^{(D)})^2 &\sim \int \frac{d^D p_E}{(2\pi)^D} \frac{B^2(p_E^2)}{[p_E^2 + B^2(p_E^2)]^2}, \\ &\propto M^D \int dp_E \frac{1}{p_E^3}. \end{aligned} \tag{5.15}$$

This suggests that the dynamically induced bulk Yukawa coupling $g_Y = M/F_\pi^{(D)}$ can be made finite even in the "infinite cutoff limit" $\Lambda \to \infty$.[5] This is in contrast with perturbation theory where the gauge theory in D (> 4) dimensions is obviously nonrenormalizable. This situation is similar to the renormalizability of the gauged NJL model [22].

6 Chiral fermion on the 3-brane

We have investigated so far the possibility of DχSB in the bulk. Since a chiral fermion in the bulk ($D > 4$) has four or more components, it is nontrivial to obtain a four-

[5]This statement is of course rather formal in the sense that κ_D in Eq. (3.17) is actually not an arbitrary adjustable parameter and hence cannot be fine tuned to $\kappa_D^{\rm crit}$, $\kappa_D \to \kappa_D^{\rm crit}$, to make the dynamical mass M finite through Eq. (4.21) in that limit.

dimensional chiral fermion with two components as an effective theory. For such a purpose, we need to compactify the extra dimensions on an orbifold, in which unwanted components are projected out by its boundary conditions [7]. In this section we describe a systematic procedure to find such orbifold compactifications.

We start with the minimal case $D = 6$ for simplicity. The chiral projection operators in six dimensions are given by

$$\frac{1 \pm \Gamma_{A,7}}{2}, \qquad \Gamma_{A,7} \equiv \Gamma^0\Gamma^1\Gamma^2\Gamma^3\Gamma^5\Gamma^6, \tag{6.1}$$

and the chiral fermions $\psi_\pm$ obey

$$\Gamma_{A,7}\psi_\pm = \pm\psi_\pm. \tag{6.2}$$

Hereafter we argue only ψ_+, the chiral fermion with positive chirality in the bulk. It is easy to extend our arguments to the case of ψ_-.

We next decompose the space-time coordinate into conventional and extra dimensions:

$$x^M = (x^\mu, y^m), \qquad \mu = 0, 1, 2, 3, \qquad m = 5, 6, \tag{6.3}$$

and assume a torus compactification,

$$\psi_+(x, y^5, y^6) = \psi_+(x, y^5 + 2\pi R, y^6) = \psi_+(x, y^5, y^6 + 2\pi R), \tag{6.4}$$

where the radii of the fifth and sixth dimensions are assumed to be the same (denoted by R) for simplicity. The chiral fermion in $D = 6$ is then decomposed into KK modes:

$$\psi_+(x, y) = \sum_{k_5,k_6} \psi_+^{k_5k_6}(x) \exp\left[i\frac{k_5y^5 + k_6y^6}{R}\right]. \tag{6.5}$$

We next introduce the four-dimensional chirality matrix $\Gamma_{A,5} \equiv i\Gamma^0\Gamma^1\Gamma^2\Gamma^3$. It is easy to show several identities:

$$[\Gamma_{A,5}, \Gamma_{A,7}] = 0, \quad \Gamma_{A,5}\Gamma_{A,5} = 1, \quad \mathrm{tr}\left[\Gamma_{A,5}\frac{1 \pm \Gamma_{A,7}}{2}\right] = 0, \tag{6.6}$$

which indicate that $\Gamma_{A,5}$ and $\Gamma_{A,7}$ are simultaneously diagonalizable, eigenvalues of $\Gamma_{A,5}$ are ± 1, and the sum of eigenvalues of $\Gamma_{A,5}$ is zero for a chiral fermion in the six-dimensional bulk. It is therefore evident that the zero mode ψ_+^{00} in this torus compactification is vectorlike in its four-dimensional effective theory. We need to eliminate unwanted components of the fermion on the four-dimensional brane by imposing a certain orbifold symmetry.

It should be noted, however, that the "parity" of extra dimensions does not suit our purpose, because it is explicitly violated in the chiral theory of the bulk.[6] We then

[6] CP is also violated in the six-dimensional bulk, since charge conjugation does not flip chirality in $D = 4k + 2$ dimensions.

try to adopt rotation in the extra dimensions by the angle π:[7]

$$\begin{aligned}\psi'(x, y^5, y^6) &= \exp\left[\frac{i}{2}\Sigma^{56}\pi\right]\psi(x, -y^5, -y^6) \\ &= i\Sigma^{56}\psi(x, -y^5, -y^6),\end{aligned} \tag{6.7}$$

with Σ^{MN} being defined by

$$\Sigma^{MN} \equiv \frac{i}{2}[\Gamma^M, \Gamma^N]. \tag{6.8}$$

There are two possible boundary conditions of this orbifold:

$$\psi_+(x, y^5, y^6) = (-1)^n\Sigma^{56}\psi_+(x, -y^5, -y^6), \qquad n = 0 \text{ or } 1, \tag{6.9}$$

which leads to the constraint for the zero mode fermion

$$\psi_+^{00}(x) = (-1)^n\Sigma^{56}\psi_+^{00}(x). \tag{6.10}$$

Noting the identity $\Sigma^{56} = -\Gamma_{A,5}\Gamma_{A,7}$, we can rewrite Eq. (6.10) into the conditions of the chiral fermion on the four dimensional brane:

$$\Gamma_{A,5}\psi_+^{00}(x) = (-1)^{n+1}\psi_+^{00}(x). \tag{6.11}$$

The chirality on the brane is determined by the choice of the boundary condition, $n = 0$ or 1, in Eq. (6.9)

It should be emphasized here that our procedures described in this section do not depend on a particular choice of the representation of the Clifford algebra. We can easily generalize our arguments to an orbifold compactification from $D = 2(k+1)$ into $D = 2k$ dimensions. By applying these procedures repeatedly, we are thus able to obtain orbifold compactification starting from a bulk chiral theory of $D = 2k$ ($k \geq 3$) into a brane chiral theory with four dimensions.

7 Effective gauge coupling

Although the $\overline{MS}$-scheme has been widely adopted for running gauge coupling in the improved ladder approximation, it is worth investigating yet another choice, "effective" gauge coupling g_{eff}, which is closely related to the gauge boson propagator and its momentum. For this purpose, we evaluate the one-loop gauge boson propagator in the truncated KK effective theory on the 3-brane, and derive a relation between the effective and the $\overline{MS}$ couplings.

[7] It is also possible to use $\pi/2$ rotation to define an orbifold, which keeps chirality on the four-dimensional brane.

The effective gauge coupling $g_{\rm eff}$ on the 3-brane is defined by[8]

$$\frac{-i}{g_{\rm eff}^2(q^2)} D^{-1}_{\mu\nu}(q) \equiv \frac{-i}{g_0^2} D^{-1}_{(0)\mu\nu}(q) - (q^2 g_{\mu\nu} - q_\mu q_\nu)\Pi(q^2) \tag{7.1}$$

with g_0 being the bare gauge coupling, and the (four-dimensional) gauge boson propagators are given by

$$D_{(0)\mu\nu}(q) = \frac{-i}{q^2}\left(g_{\mu\nu} - (1-\xi_0)\frac{q_\mu q_\nu}{q^2}\right), \qquad D_{\mu\nu}(q) = \frac{-i}{q^2}\left(g_{\mu\nu} - (1-\xi_{\rm eff}(q^2))\frac{q_\mu q_\nu}{q^2}\right). \tag{7.2}$$

Equation (7.1) reads

$$\frac{1}{g_{\rm eff}^2(q^2)} = \frac{1}{g_0^2} - \Pi(q^2). \tag{7.3}$$

The vacuum polarization function $\Pi(q^2)$ can be decomposed into loops of each KK mode at the one-loop level:

$$\Pi(q^2) = \sum_{\vec{n}} \Pi(q^2, m_{\vec{n}}^2), \qquad m_{\vec{n}}^2 = \frac{|\vec{n}|^2}{R^2}. \tag{7.4}$$

In order to calculate the relation between the effective and the $\overline{MS}$ couplings, we next evaluate $\Pi(q^2, m_{\vec{n}}^2)$ using dimensional regularization ($d \equiv 4+\epsilon$),

$$\Pi(q^2, m^2) = C_G\left[4 I_g(q^2, m^2) + (2-D) I_b(q^2, m^2)\right] - 2\eta T_R N_f I_f(q^2, m^2), \tag{7.5}$$

where we used notations introduced in Section 2 and

$$\begin{aligned} I_g(q^2, m^2) &\equiv \frac{\Gamma(2-d/2)}{(4\pi)^{d/2}} \int_0^1 dx \left[m^2 - x(1-x)q^2\right]^{d/2-2}, \\ I_b(q^2, m^2) &\equiv \frac{\Gamma(2-d/2)}{2(4\pi)^{d/2}} \int_0^1 dx (2x-1)^2 \left[m^2 - x(1-x)q^2\right]^{d/2-2}, \\ I_f(q^2, m^2) &\equiv \frac{\Gamma(2-d/2)}{(4\pi)^{d/2}} \int_0^1 dx x(1-x) \left[m^2 - x(1-x)q^2\right]^{d/2-2}. \end{aligned}$$

The counterterm for the $\overline{MS}$ coupling[9] in the truncated KK effective theory is given by

$$\frac{1}{g_{\overline{MS}}^2(\mu)} = \frac{1}{g_0^2} - \sum_{\vec{n}}^{m_{\vec{n}} > \mu} \Pi(q^2 = 0, m_{\vec{n}}^2) + \sum_{\vec{n}}^{m_{\vec{n}} \le \mu} \frac{\Gamma(2-d/2)}{(4\pi)^{d/2}} b' \mu^{d-4}, \tag{7.6}$$

[8] We use the background gauge-fixing method throughout this section. The Ward-Takahashi identities of non-Abelian gauge theory are QED-like and keep manifest gauge invariance in this gauge fixing.

[9] Strictly speaking, Eq. (7.6) is evaluated in the modified dimensional reduction scheme [36].

where the term $\sum_{\vec{n}}^{m_{\vec{n}}>\mu} \Pi(q^2=0, m_{\vec{n}}^2)$ comes from the loop of KK modes heavier than the renormalization scale μ. This term is independent of μ and therefore does not affect the RGE for the gauge coupling, in accordance with the decoupling theorem that is assumed in the truncated KK effective theory.

Taking the $d \to 4$ limit we now obtain

$$\frac{1}{g_{\rm eff}^2(q^2)} = \frac{1}{g_{\overline{MS}}^2(\mu)} - \sum_{\vec{n}}^{m_{\vec{n}}>\mu} \Pi_{>}(q^2, m_{\vec{n}}^2) - \sum_{\vec{n}}^{m_{\vec{n}}\le\mu} \Pi_{<}(q^2, m_{\vec{n}}^2; \mu), \tag{7.7}$$

where $\Pi_>$ and $\Pi_<$ are given by

$$\begin{aligned}
(4\pi)^2 \Pi_{>}(q^2, m^2) &\equiv -C_G \int_0^1 dx \left[4 + \frac{2-D}{2}(2x-1)^2\right] \ln\left(1 - \frac{q^2}{m^2}x(1-x)\right) \\
&\quad + 2\eta T_R N_f \int_0^1 dx x(1-x) \ln\left(1 - \frac{q^2}{m^2}x(1-x)\right), \qquad (7.8) \\
(4\pi)^2 \Pi_{<}(q^2, m^2; \mu) &\equiv -C_G \int_0^1 dx \left[4 + \frac{2-D}{2}(2x-1)^2\right] \ln\left(\frac{m^2 - q^2 x(1-x)}{\mu^2}\right) \\
&\quad + 2\eta T_R N_f \int_0^1 dx x(1-x) \ln\left(\frac{m^2 - q^2 x(1-x)}{\mu^2}\right). \qquad (7.9)
\end{aligned}$$

Note here that the μ dependence in the right-hand side of Eq. (7.7) cancels exactly. We also introduce a *dimensionless* effective gauge coupling of the *bulk* gauge theory defined in a similar manner to Eq. (2.2),

$$\hat{g}_{\rm eff}^2(q^2) = \frac{(2\pi R\sqrt{-q^2})^\delta}{n} g_{\rm eff}^2(q^2). \tag{7.10}$$

Using approximations described in Appendix C, we find

$$\frac{1}{\hat{g}_{\rm eff}^2(q^2)} \simeq \frac{\lambda}{\hat{g}_{\overline{MS}}^2(\sqrt{-\lambda q^2})} + \frac{1}{(4\pi)^3}\left[-\frac{3}{5}C_G + \frac{\eta}{15}T_R N_f\right] \ln\left(\frac{-\lambda q^2}{\Lambda^2}\right) \tag{7.11}$$

for the bulk gauge theory in $D=6$ dimensions. Here λ is given by

$$\lambda = \exp\left[\frac{C_G\left(-8 - \frac{4}{9}(2-D)\right) + \frac{5}{9}\eta T_R N_f}{-b'}\right]. \tag{7.12}$$

In the analysis of the SD equation based on $g_{\rm eff}$, we adopt the effective coupling $\hat{g}_{\rm eff}^2$ Eq. (7.11) [instead of $\hat{g}_{\overline{MS}}^2$ in Eq. (2.14)] in the formula for the improved ladder approximation Eq. (3.15).

Several comments are in order.

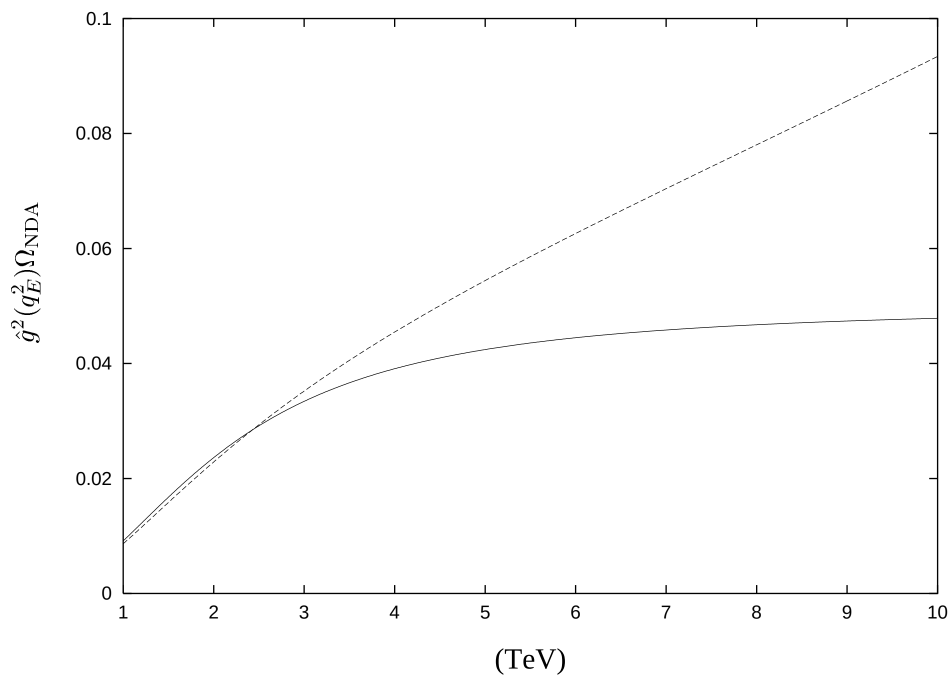

Figure 6: The graph of the dimensionless gauge coupling with $C_G = 3$, $N_f = 0$, $R^{-1} = 1$ TeV, $\Lambda = 10$ TeV, $\alpha_{\overline{MS}}(M_Z) = 0.1$. The solid line and the dashed line represent the $\overline{MS}$ coupling and the effective coupling of Eq. (7.11), respectively.

a) The decoupling theorem is violated in the effective coupling Eq. (7.11), since it depends explicitly on the ultraviolet cutoff Λ. This result comes from the nonrenormalizability of the six-dimensional bulk gauge theory.

b) The effective coupling is larger than the $\overline{MS}$ coupling by approximately a factor of λ^{-1}. (See also Fig. 6.) If we adopt $\hat{g}_{\rm eff}$ instead of $\hat{g}_{\overline{MS}}$ in the improved ladder approximation, there is a chance that the bulk QCD coupling even in six dimensions can be strong enough to cause DχSB in the bulk under certain conditions.

c) There still exists an *upper bound* on $\hat{g}_{\rm eff}$ similar to the nontrivial UV fixed point, which is roughly proportional to the UV fixed point in the $\overline{MS}$ scheme. (See Appendix C for a detailed discussion.) It is therefore still a nontrivial question whether DχSB occurs or not in the bulk gauge theories even if we adopt $\hat{g}_{\rm eff}$ in the improved ladder SD equation.

d) We can define an analogue of the "β function" for "bare coupling" $\hat{g}_\Lambda \equiv \hat{g}_{\rm eff}(q^2 = -\Lambda^2)$. (See Appendix C.) The upper bound of $\hat{g}_{\rm eff}$ can be regarded as an UV fixed point of such a "β function" and therefore independent of the choice of the cutoff scale Λ.

In fact the finite renormalization effect is the largest uncertainty of our analysis based on the improved ladder SD equation, compared with other uncertainties such as the nonladder effects, higher-order corrections, etc. A detailed analysis of the improved

ladder SD equation with $\hat{g}_{\text{eff}}$ will be presented elsewhere [37].

8 Summary and discussions

We have studied dynamical issues of the ACDH version [7] of the TMSM [1, 2, 3, 5] within the framework of the improved ladder SD equation. Based on the truncated KK effective theory [17], we found that D-dimensional non-Abelian gauge theories with compactified extra dimensions possess a nontrivial UV fixed point. We then evaluated the UV fixed point by using the one-loop RGE, assuming its nonperturbative existence. Although the SM couplings in the D-dimensional bulk generally become strong beyond the compactification scale, the (dimensionless) bulk coupling cannot grow beyond the UV fixed point and hence it is highly nontrivial whether or not DχSB really takes place.

For the simplest scenario of ACDH with the massless gauge bosons and third family quarks and leptons living in the D-dimensional bulk and the rest in the four-dimensional brane (3-brane), we have the UV fixed points Eqs. (4.6),(4.8):

$$\kappa_6 = 0.091, \quad \kappa_8 = 0.242 \tag{8.1}$$

for bulk dimensions of six and eight, respectively.

On the other hand, the improved ladder SD equation in D (> 4) dimensions yields the critical points in six/eight dimensions as Eqs. (4.5),(4.7):

$$\kappa_6^{\text{crit}} = 0.122, \quad \kappa_8^{\text{crit}} = 0.146. \tag{8.2}$$

These results are qualitatively consistent with a naive dimensional analysis. The ACDH scenario thus can work for $D = 8$ but not for $D = 6$ if we take the results Eq. (8.1) and Eq. (8.2) at face value. It should be emphasized, however, that our analysis is based on the ladder approximation. We would certainly need further investigation to incorporate non-ladder effects in order to evaluate the critical value more accurately.

We also discussed some subtlety about the "improved" ladder SD equation by replacing the $\overline{MS}$ running coupling by the effective coupling including the finite renormalization effects. This makes attractive forces somewhat larger than in $\overline{MS}$ coupling, so that the condensate can occur more easily. In the case of the ACDH scenario, top condensation may be possible due to effects of finite renormalization even in six dimensions, since the coupling has a chance to increase over the critical point *for sufficiently large cutoff*.

However, if the cutoff is too large, then the $U(1)$ coupling dominates the QCD coupling so that the MAC favors other channels (tau lepton condensate) than the top quark condensate. We then obtain some conditions for the "effective (phenomenological) cutoff" (Λ) where the bulk QCD and hypercharge couplings are aligned in the MAC in such a way that only the top quark condenses while others (bottom, etc.) do not. Another constraint comes from the top quark mass which is related to the decay

constant $F_\pi^{(D)}$ in D dimensions through the PS formula, Eq. (5.15). Thus it is related to the weak scale $F_\pi = 246$ GeV as

$$F_\pi^2 = \frac{(2\pi R)^\delta}{n}(F_\pi^{(D)})^2. \tag{8.3}$$

These matters will be dealt with in a forthcoming paper [37].

The salient feature of the improved ladder SD equation in D (> 4) dimensions is its approximate scale invariance. The reason is the followings. The bulk dimensionful coupling can be written as the dimensionless coupling multiplied by a factor having dimensions carried by the renormalization point μ [see Eq. (2.11)], which is then traded for the momentum in the running coupling in the improved ladder SD equation, and moreover the running coupling quickly increases up to the UV fixed point. Hence the SD equation can be well approximated by the coupling at the fixed point. Then the resulting SD equation Eq. (3.16) has no scale parameters except for the cutoff.

This is the very reason why we obtained the essential-singularity scaling of the conformal phase transition, Eq. (4.21), with the analytical result for the critical point Eq. (4.18)

$$\kappa_D^{\rm crit} = \frac{D-2}{8(D-1)}, \tag{8.4}$$

which was derived through certain approximations and is consistent with the numerical result above.

The essential-singularity scaling gives us the possibility to have a large hierarchy between the weak scale and the cutoff without fine tuning. Here we note that κ_D is not an arbitrary parameter but a definite number once the model is set up. We should therefore note that it is impossible to take the cutoff infinitely large.

In a realistic model based on the ACDH scenario, however, the bulk gauge coupling of QCD is determined through matching with the QCD on the 3-brane at the compactification scale R^{-1}. The bulk coupling grows at high energy toward the UV fixed point and can exceed the critical coupling only for a certain cutoff ("critical cutoff"). When we tune the cutoff very close to the critical one, the SD equation yields a very small dynamical mass compared with the cutoff. We are thus able to determine the value of the cutoff, which enables us to evaluate the low-energy predictions of the ACDH scenario (e.g., m_t and m_H) more accurately.

Moreover, we had a very large anomalous dimension Eq. (5.14):

$$\gamma_m = \frac{D}{2} - 1, \tag{8.5}$$

which happens to coincide with the cases for $D \leq 4$, i.e., the quenched ladder SD equation (with nonrunning or walking/standing coupling) for $D = 4$ ($\gamma_m = 1$) and also with the improved ladder SD equation for $D = 3$ QED ($\gamma_m = 1/2$) where the running coupling has an infrared fixed point. In all the cases including $D \leq 4$, the SD equation has scale invariance at the fixed point.

Acknowledgments

We would like to thank Howard Georgi, Valery Gusynin, Masayasu Harada, Yoshio Kikukawa, Volodya Miransky, Takeo Moroi, and Masahiro Yamaguchi for useful discussions. K.Y. thanks Howard Georgi for hospitality at Harvard where a part of this work was done. This work is supported by Grant-in-Aid for Scientific Research (B) #11695030 (K.Y.), (A) #12014206 (K.Y.), the JSPS Research Fellowships for Young Scientists #01170 (M.H.), and the Oversea Research Scholar Program of the Monbusho (Ministry of Education, Science, Sports and Culture) (K.Y.).

A Angular integrals in the ladder SD equations

The momentum integrals of the SD equations Eq. (3.5) and Eq. (3.6) can be decomposed into polar and angular integrals,

$$\int \frac{d^D q_E}{(2\pi)^D} F(p_E^2, q_E^2, p_E \cdot q_E) = C_D \int_0^{\Lambda^2} dy\, y^{D/2-1} \int_0^{\pi} d\theta \sin^{D-2}\theta F(x, y, \sqrt{xy}\cos\theta), \quad \text{(A.1)}$$

with $x \equiv p_E^2$, $y \equiv q_E^2$, and C_D defined by $C_D \equiv \Omega_{\mathrm{NDA}}/B(1/2, D/2-1/2)$. In order to evaluate the angular integral $d\theta$, we define the integral

$$I(\mu,\nu,\rho;z) \equiv \int_0^{\pi} d\theta \frac{\sin^{2\nu+1}\theta \cos^{\rho}\theta}{(z-\cos\theta)^{\mu+\nu+1}}. \quad \text{(A.2)}$$

It is easy to see that the angular integrals in Eq. (3.5) and Eq. (3.6) can be expressed in terms of $I(\mu,\nu,0;z)$ and $I(\mu,\nu,1;z)$ with $z \equiv (x+y)/(2\sqrt{xy})$. We obtain [25]

$$\begin{aligned} A(x) &= 1 + \frac{C_F g_D^2}{x} C_D \int_0^{\Lambda^2} dy y^{D/2-1} \frac{A(y)}{A^2 y + B^2} \\ &\quad \times \left\{ \frac{D-1-\xi}{2} I(\frac{3}{2}-\frac{D}{2}, \frac{D}{2}-\frac{3}{2}, 1; z) - \frac{1-\xi}{2} I(\frac{3}{2}-\frac{D}{2}, \frac{D}{2}-\frac{1}{2}, 0; z) \right\}, \quad \text{(A.3)} \\ B(x) &= (D-1+\xi) C_F g_D^2 C_D \int_0^{\Lambda^2} dy y^{D/2-1} \frac{B(y)}{A^2 y + B^2} \frac{1}{2\sqrt{xy}} I(\frac{3}{2}-\frac{D}{2}, \frac{D}{2}-\frac{3}{2}, 0; z). \end{aligned}$$

(A.4)

Using the relation

$$I(\mu,\nu,1;z) = \frac{1}{2\nu+2} \int_0^{\pi} d\theta \frac{1}{(z-\cos\theta)^{\mu+\nu+1}} \frac{d}{d\theta}\left[\sin^{2\nu+2}\theta\right] = \frac{\mu+\nu+1}{2\nu+2} I(\mu,\nu+1,0;z),$$

(A.5)

Eq. (A.3) can be further simplified:

$$A(x) = 1 + \frac{\xi}{2}\frac{D-2}{D-1}\frac{C_F g_D^2}{x} C_D \int_0^{\Lambda^2} dy y^{D/2-1} \frac{A(y)}{A^2 y + B^2} I(\frac{3}{2}-\frac{D}{2}, \frac{D}{2}-\frac{1}{2}, 0; z). \quad \text{(A.6)}$$

It should be noted that $A(x) = 1$ holds for arbitrary dimensions in the Landau gauge $\xi = 0$ [25].

The integral $I(\mu, \nu, 0; z)$ was given for certain integer dimensions in Ref. [25] and now is expressed in terms of the hypergeometric function $F(\alpha, \beta, \gamma; z)$ for arbitrary D:

$$I(\mu, \nu, 0; z) = \frac{2^{\mu+\nu+1}\sqrt{\pi}\,\Gamma(\nu+1)}{\tilde{z}^{\mu+\nu+1}\Gamma(\nu+\frac{3}{2})} F(\mu+\nu+1, \mu+\frac{1}{2}, \nu+\frac{3}{2}; \tilde{z}^{-2}), \tag{A.7}$$

with

$$\tilde{z} \equiv z + \sqrt{z^2 - 1} = \frac{\max(x, y)}{\sqrt{xy}}, \qquad \tilde{z}^{-2} = \frac{\min(x, y)}{\max(x, y)}. \tag{A.8}$$

We thus obtain the integral kernel K_A,

$$K_A(x, y) = \tilde{z}^{-2} F(2, 2 - D/2, D/2 + 1; \tilde{z}^{-2}), \tag{A.9}$$

and the integral kernel K_B [38],

$$K_B(x, y) = \frac{1}{\max(x, y)} F(1, 2 - D/2, D/2; \tilde{z}^{-2}). \tag{A.10}$$

Using the Taylor expansion of the hypergeometric function

$$F(\alpha, \beta, \gamma; z) = \sum_{\ell=0}^{\infty} \frac{(\alpha)_\ell (\beta)_\ell}{(\gamma)_\ell} \frac{z^\ell}{\ell!}, \qquad (\alpha)_\ell \equiv \alpha(\alpha+1)(\alpha+2)\cdots(\alpha+\ell-1),$$

we obtain

$$\begin{aligned} K_A(x, y) &\equiv \frac{y}{x} \sum_{\ell=0}^{\delta/2} \frac{(-\delta/2)_\ell (\ell+1)}{(\delta/2+3)_\ell} \left(\frac{y}{x}\right)^\ell \theta(x-y) + (x \leftrightarrow y), & \text{(A.11)} \\ K_B(x, y) &\equiv \frac{1}{x} \sum_{\ell=0}^{\delta/2} \frac{(-\delta/2)_\ell}{(\delta/2+2)_\ell} \left(\frac{y}{x}\right)^\ell \theta(x-y) + (x \leftrightarrow y) & \text{(A.12)} \end{aligned}$$

for even dimensions $D = 4 + \delta \geq 4$.

B The NJL model in D (> 4) dimensions

We consider the Nambu–Jona-Lasinio (NJL) model[10] in $D(> 4)$ dimensions,

$$\mathcal{L} = \bar{\psi} i \Gamma^M \partial_M \psi + \frac{G}{2N} (\bar{\psi}\psi)^2. \tag{B.1}$$

[10] In order to avoid the complexity associated with the definition of continuous chiral symmetry in D dimensions, we discuss in this Appendix the NJL model that has only discrete chiral symmetry (it may be called the "Gross-Neveu" model.)

The gap equation is obtained from the self-consistency condition for the dynamical mass m. In the large N limit, we find

$$\begin{aligned} m &= \frac{\eta\, G\Lambda^{D-2}}{(4\pi)^{D/2}\Gamma(D/2)} \int_0^{\Lambda^2} dp_E^2 \left(\frac{p_E^2}{\Lambda^2}\right)^{D/2-1} \frac{m}{p_E^2+m^2}, \\ &= g\int_0^1 dz\, z^{D/2-1}\frac{m}{z+m^2/\Lambda^2}, \end{aligned} \tag{B.2}$$

where η $(= 2^{D/2})$ represents the dimension of the spinor representation of $SO(1, D-1)$. The dimensionless NJL coupling g is defined by $g \equiv (4\pi)^{-D/2}\eta G\Lambda^{D-2}/\Gamma(D/2)$. Expanding the integrand of Eq. (B.2) in terms of m/Λ, we obtain

$$\frac{1}{g} = \frac{1}{D/2-1} - \frac{1}{D/2-2}\frac{m^2}{\Lambda^2} + \cdots .$$

The scaling behavior of the NJL model in D (> 4) dimensions is then given by

$$\frac{1}{g_{crit}} - \frac{1}{g} = \frac{2}{D-4}\frac{m^2}{\Lambda^2}, \qquad g_{crit} \equiv D/2-1. \tag{B.3}$$

In order to obtain hierarchy between m and Λ, we thus need a fine tuning of the NJL coupling strength at the precision of the $(m/\Lambda)^2$ level *irrespectively of D for $D > 4$.* The situation contrasts with the NJL model in dimensions less than four where the NJL coupling needs to be close to its critical point at the precision of $(m/\Lambda)^{D-2}$.

C Approximate formulas for $g_{\rm eff}$

Equation (7.7) can be further simplified by making several approximations. We first concentrate our attention on $\Pi_<$. This term depends on the renormalization scale μ and therefore it can be minimized by taking an optimized choice of μ. We assume that the appropriate μ^2 is proportional to $-q^2$:

$$\mu^2 = -\lambda q^2, \tag{C.1}$$

with λ being a constant which we will determine below. Since the mass of the KK mode $m_{\vec{n}}$ is always lighter than the renormalization scale μ in $\Pi_<$, we can safely neglect $m_{\vec{n}}$ in the following analysis. It is straightforward to evaluate $\Pi_<$,

$$(4\pi)^2\Pi_<(q^2, 0; \mu = \sqrt{-\lambda q^2}) = C_G\left[8 + \frac{4}{9}(2-D)\right] - \frac{5}{9}\eta T_R N_f - b' \ln\lambda. \tag{C.2}$$

This term vanishes if we take the optimized value of λ:

$$\ln\lambda = \frac{C_G\left(-8 - \frac{4}{9}(2-D)\right) + \frac{5}{9}\eta T_R N_f}{-b'}. \tag{C.3}$$

We next turn to $\Pi_>$. The KK mass is always heavier than the renormalization scale μ in this term, while μ is proportional to q^2 in the previous optimization procedure. We therefore expand $\Pi_>$ in terms of the powers of $-q^2/m_{\vec{n}}^2$. We find

$$(4\pi)^2\Pi_>(q^2, m^2) = -C_G\left[\frac{2}{3} + \frac{2-D}{60}\right]\left(\frac{-q^2}{m^2}\right) + \frac{\eta}{15}T_R N_f\left(\frac{-q^2}{m^2}\right) + \mathcal{O}\left(\left(\frac{-q^2}{m^2}\right)^2\right). \tag{C.4}$$

The sum of the KK modes can be approximated by replacing it with an integral:

$$\sum_{\vec{k}}^{m_{\vec{k}}>\mu} \to \frac{1}{n}\frac{2\pi^{\delta/2}}{\Gamma(\delta/2)}R\int_\mu^\Lambda dm(Rm)^{\delta-1}, \tag{C.5}$$

which leads to

$$\sum_{\vec{k}}^{m_{\vec{k}}>\mu} \Pi_>(q^2, m_{\vec{k}}^2) \simeq \frac{\pi R^2}{(4\pi)^2 n}\left[-\frac{3}{5}C_G + \frac{\eta}{15}T_R N_f\right](-q^2)\ln\frac{\Lambda^2}{\mu^2} \tag{C.6}$$

for $D = 4+\delta$, $\delta = 2$. Combining Eqs. (C.3), (C.6) and (7.10), it is now easy to obtain Eq. (7.11). The validity of Eq. (7.11) can be confirmed also numerically. (See Fig.7.) It should be noted that the approximation of Eq. (C.4) is not justified for $\lambda \ll 1$, however. In order to obtain the upper bound of $\hat{g}_{\rm eff}$ including such a possibility, we next evaluate the effective coupling without use of the approximations of Eq. (C.2) and Eq. (C.4). Using the approximation Eq. (C.5), we obtain a formula for the effective gauge coupling strength in six dimensions:

$$\begin{aligned}\frac{1}{\hat{g}_{\rm eff}^2(q^2)} &= \frac{\mu^2}{(-q^2)}\left(\frac{1}{\hat{g}_{\overline{MS}}^2(\mu)} + \frac{b'}{(4\pi)^3}\right) \\ &\quad + \frac{1}{(4\pi)^3}\left[K_g(q^2,\Lambda^2) + K_b(q^2,\Lambda^2) + K_f(q^2,\Lambda^2)\right],\end{aligned} \tag{C.7}$$

with

$$\begin{aligned}K_g(q^2,\Lambda^2) &\equiv 4C_G\left(\frac{5}{18} + \frac{1}{6}\ln\frac{\Lambda^2}{(-q^2)} + \frac{\Lambda^2}{(-q^2)}\tilde{K}_g(q^2,\Lambda^2)\right), \\ K_b(q^2,\Lambda^2) &\equiv -2C_G\left(\frac{31}{450} + \frac{1}{30}\ln\frac{\Lambda^2}{(-q^2)} + \frac{\Lambda^2}{(-q^2)}\tilde{K}_b(q^2,\Lambda^2)\right), \\ K_f(q^2,\Lambda^2) &\equiv -2\eta T_R N_f\left(\frac{47}{900} + \frac{1}{30}\ln\frac{\Lambda^2}{(-q^2)} + \frac{\Lambda^2}{(-q^2)}\tilde{K}_f(q^2,\Lambda^2)\right).\end{aligned}$$

The functions $\tilde{K}_g$, $\tilde{K}_b$, $\tilde{K}_f$ are defined by

$$\begin{aligned}\tilde{K}_g(q^2,\Lambda^2) &\equiv \int_0^1 dx f(q^2,\Lambda^2,x), \\ \tilde{K}_b(q^2,\Lambda^2) &\equiv \int_0^1 dx(2x-1)^2 f(q^2,\Lambda^2,x), \\ \tilde{K}_f(q^2,\Lambda^2) &\equiv \int_0^1 dx x(1-x) f(q^2,\Lambda^2,x),\end{aligned}$$

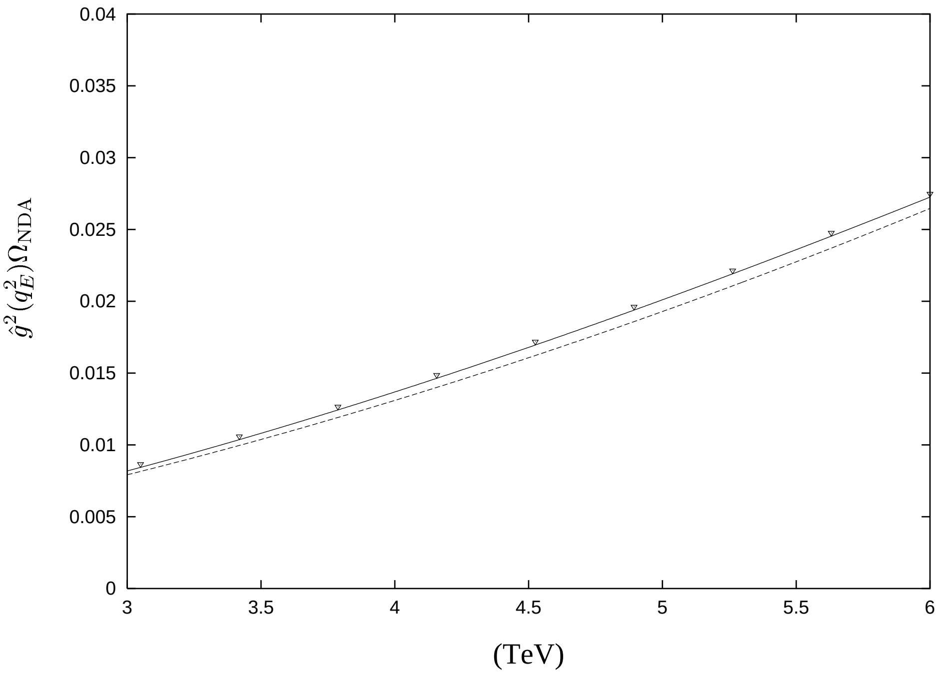

Figure 7: Graphs of the dimensionless gauge couplings. The solid line and the dashed line represent the effective coupling of Eq. (C.7) and Eq. (7.11), respectively. We also plot with the white triangles the coupling directly calculated from the definition of Eq. (7.7) without using approximation Eq. (C.5). In this graph, we took $C_G = 3$, $N_f = 0$, $R^{-1} = 3$ TeV, $\Lambda = 6$ TeV.

with

$$f(q^2, \Lambda^2, x) \equiv (1 - x(1-x)\frac{q^2}{\Lambda^2}) \ln\left(1 - \frac{q^2}{\Lambda^2} x(1-x)\right).$$

The integrals can be performed easily and we obtain (in the Euclidean region $q^2 < 0$)

$$\begin{aligned}
\tilde{K}_g(q^2, \Lambda^2) &= -\frac{4}{3} + \frac{5}{18}\frac{q^2}{\Lambda^2} + \frac{1}{3}\left(4 - \frac{q^2}{\Lambda^2}\right)^{3/2}\left(\frac{\Lambda^2}{-q^2}\right)^{1/2} \tanh^{-1}\sqrt{\frac{-q^2}{4\Lambda^2 - q^2}}, \\
\tilde{K}_b(q^2, \Lambda^2) &= \frac{16}{15}\frac{\Lambda^2}{q^2} - \frac{28}{45} + \frac{31}{450}\frac{q^2}{\Lambda^2} + \frac{1}{15}\left(4 - \frac{q^2}{\Lambda^2}\right)^{5/2}\left(\frac{\Lambda^2}{-q^2}\right)^{3/2} \tanh^{-1}\sqrt{\frac{-q^2}{4\Lambda^2 - q^2}}, \\
\tilde{K}_f(q^2, \Lambda^2) &= -\frac{4}{15}\frac{\Lambda^2}{q^2} - \frac{8}{45} + \frac{47}{900}\frac{q^2}{\Lambda^2} \\
&\quad -\frac{1}{15}\left(4 - \frac{q^2}{\Lambda^2}\right)^{3/2}\left(1 + \frac{q^2}{\Lambda^2}\right)\left(\frac{\Lambda^2}{-q^2}\right)^{3/2} \tanh^{-1}\sqrt{\frac{-q^2}{4\Lambda^2 - q^2}}.
\end{aligned}$$

It is evident that $\hat{g}_{\rm eff}$ reaches its maximum at $q^2 = -\Lambda^2$. (See Fig. 7.) We obtain

$$K \equiv \sum_{i=g,b,f} K_i(-\Lambda^2, \Lambda^2) = C_G \left(-\frac{88}{45} + \frac{10\sqrt{5}}{3} \tanh^{-1} \frac{1}{\sqrt{5}} \right) - \frac{8\eta T_R}{45} N_f. \qquad \text{(C.8)}$$

Equation (C.7) thus leads to an upper bound on $\hat{g}_{\rm eff}$,

$$\hat{g}^2_{\rm eff}(q^2) < \frac{(4\pi)^3}{K} \qquad \text{for } 0 \le -q^2 \le \Lambda^2, \qquad \text{(C.9)}$$

where we have assumed that the $\overline{MS}$ coupling is below its UV fixed point,

$$\hat{g}^2_{\overline{MS}} < g_*^2 = \frac{(4\pi)^3}{-b'}. \qquad \text{(C.10)}$$

It should be emphasized that Eq. (C.8) is independent of the cutoff Λ and thus the upper bound Eq. (C.9) can be adopted for arbitrary Λ. In order to clarify the point, it is illuminating to define $\hat{g}_\Lambda$ by

$$\hat{g}^2_\Lambda \equiv \hat{g}^2_{\rm eff}(q^2 = -\Lambda^2). \qquad \text{(C.11)}$$

The coupling $\hat{g}_\Lambda$ can be regarded as a "bare parameter" of the present model. An analogue of the "β function" for $\hat{g}_\Lambda$ is then given by

$$\beta(\hat{g}_\Lambda) \equiv \Lambda \frac{d}{d\Lambda} \hat{g}_\Lambda = \hat{g}_\Lambda - \frac{K}{(4\pi)^3} \hat{g}^3_\Lambda. \qquad \text{(C.12)}$$

The upper limit $(4\pi)^3/K$ is thus given by the UV fixed point of the "β function" Eq. (C.12).

Numerically we obtain $K \simeq 1.63 C_G - 0.71 T_R N_f$. For large $-b'$ or large C_G, we thus find that the upper bound is roughly proportional to the UV fixed point in the $\overline{MS}$ scheme,

$$\frac{(4\pi)^3}{K} \simeq 2 \frac{(4\pi)^3}{-b'} = 2 g_*^2. \qquad \text{(C.13)}$$

References

[1] V. A. Miransky, M. Tanabashi, and K. Yamawaki, Phys. Lett. **B 221**, 177 (1989).

[2] V. A. Miransky, M. Tanabashi, and K. Yamawaki, Mod. Phys. Lett. **A 4**, 1043 (1989).

[3] Y. Nambu, Enrico Fermi Institute Report No. 89-08, 1989; in *Proceedings of the 1989 Workshop on Dynamical Symmetry Breaking*, edited by T. Muta and K. Yamawaki (Nagoya University, Nagoya, Japan, 1990).

[4] H. Pagels and S. Stokar, Phys. Rev. **D 20**, 2947 (1979).

[5] W. A. Bardeen, C. T. Hill, and M. Lindner, Phys. Rev. **D 41**, 1647 (1990).

[6] K. Yamawaki, Prog. Theor. Phys. Suppl. **123**, 19 (1996).

[7] N. Arkani-Hamed, H. Cheng, B. A. Dobrescu, and L. J. Hall, Phys. Rev. **D 62**, 096006 (2000).

[8] B. A. Dobrescu, Phys. Lett. **B 461**, 99 (1999); hep-ph/9903407.

[9] H. Cheng, B. A. Dobrescu, and C. T. Hill, Nucl. Phys. **B 589**, 249 (2000).

[10] C. T. Hill, Phys. Lett. **266 B**, 419 (1991); Phys. Lett. **B 345**, 483 (1995).

[11] B. A. Dobrescu and C. T. Hill, Phys. Rev. Lett. **81**, 2634 (1998).

[12] N. Arkani-Hamed, S. Dimopoulos, and G. Dvali, Phys. Lett. **B 429**, 263 (1998); Phys. Rev. **D 59**, 086004 (1999); I. Antoniadis, N. Arkani-Hamed, S. Dimopoulos, and G. Dvali, Phys. Lett. **B 436**, 257 (1998).

[13] I. Antoniadis, Phys. Lett. **B 246**, 377 (1990).

[14] H. Abe, H. Miguchi, and T. Muta, Mod. Phys. Lett. **A 15**, 445 (2000).

[15] A. B. Kobakhidze, hep-ph/9904203.

[16] S. Raby, S. Dimopoulos, and L. Susskind, Nucl. Phys. **B 169**, 373 (1980).

[17] K. R. Dienes, E. Dudas, and T. Gherghetta, Phys. Lett. **B 436**, 55 (1998); Nucl. Phys. **B 537**, 47 (1999); I. Antoniadis, S. Dimopoulos, A. Pomarol, and M. Quiros, Nucl. Phys. **B 544**, 503 (1999); Z. Kakushadze, Nucl. Phys. **B 548**, 205 (1999).

[18] V. A. Miransky, Yad. Fiz. **38**, 468 (1983) [Sov. J. Nucl. Phys. **38**, 280 (1983)]; K. Higashijima, Phys. Rev. **D 29**, 1228 (1984).

[19] V.A. Miransky and K. Yamawaki, Phys. Rev. **D 55** (1997) 5051; *ibid.* **D 56**, 3768 (1997).

[20] V. A. Miransky, Nuovo Cimento, **90 A**, 149 (1985).

[21] B. Holdom, Phys. Lett. **B 150**, 301 (1985); K. Yamawaki, M. Bando, and K. Matumoto, Phys. Rev. Lett. **56**, 1335 (1986); T. Akiba and T. Yanagida, Phys. Lett. **B 169**, 432 (1986); T. Appelquist, D. Karabali, and L. C. R. Wijewardhana, Phys. Rev. Lett. **57**, 957 (1986).

[22] K.-I. Kondo, S. Shuto, and K. Yamawaki, Mod. Phys. Lett. **A 6**, 3385 (1991); K.-I. Kondo, M. Tanabashi, and K. Yamawaki, Prog. Theor. Phys. **89**, 1249 (1993); Nagoya/Chiba preprint DPNU-91-20/Chiba-EP-53 (July, 1991), Mod. Phys. Lett. **A 8**, 2859 (1993); N.V. Krasnikov, *ibid.* **A 8**, 797 (1993); M. Harada, Y. Kikukawa, T. Kugo, and H. Nakano, Prog. Theor. Phys. **92**, 1161 (1994).

[23] A. Manohar and H. Georgi, Nucl. Phys. **B 234**, 189 (1984).

[24] Z. Chacko, M.A. Luty, and E. Pontón, J. High Energy Phys. **07**, 036 (2000).

[25] K.-I. Kondo, in *Proc. 1991 Nagoya Spring School on Dynamical Symmetry Breaking, Nagoya, April 23-27, 1991,* ed. K. Yamawaki (World Scientific Pub. Co., Singapore, 1992); K.-I. Kondo, and H. Nakatani, Mod. Phys. Lett. **A 4**, 2155 (1989).

[26] Y. Kikukawa and K. Yamawaki, Phys. Lett. **B 234**, 497 (1990).

[27] M.E. Peskin, Phys. Lett. **94 B**, 161 (1980).

[28] S. Ejiri, J. Kubo, and M. Murata, Phys. Rev. **D 62**, 105025 (2000).

[29] H. Kawai, M. Nio, and Y. Okamoto, Prog. Theor. Phys. **88**, 341 (1992).

[30] T. Appelquist, K. Lane, and U. Mahanta, Phys. Rev. Lett. **61**, 1553 (1988).

[31] D. Atkinson, J. Math. Phys. **28**, 2494 (1987).

[32] T. Maskawa and H. Nakajima, Prog. Theor. Phys. **52**, 1326 (1974); *ibid.* **54**, 860 (1975); P. I. Fomin and V. A. Miransky, Phys. Lett. **B 64**, 166 (1976); R. Fukuda and T. Kugo, Nucl. Phys. **B 117**, 250 (1976).

[33] H.D. Politzer, Nucl. Phys. **B 117**, 397 (1976).

[34] T. Nonoyama and M. Tanabashi, Prog. Theor. Phys. **81**, 209 (1989).

[35] T.W. Appelquist, D. Nash, and L.C.R. Wijewardhana, Phys. Rev. Lett. **60**, 2575 (1988).

[36] W. Siegel, Phys. Lett. **84 B**, 193 (1979); D.M. Capper, D.R.T. Jones, and P. van Nieuwenhuizen, Nucl. Phys. **B 167**, 479 (1980).

[37] V. P. Gusynin, M. Hashimoto, M. Tanabashi, and K. Yamawaki, in preparation.

[38] V. P. Gusynin, A. W. Schreiber, T. Sizer and A. G. Williams, Phys. Rev. **D 60**, 065007 (1999).